This version of the manuscript is the final revised one of the published on-line J. Phycol.52,1064–1084 (2016)©2016 Phycological Society of America
https://onlinelibrary.wiley.com/doi/full/10.1111/jpy.12464
DOI: 10.1111/jpy.124641064

Ostreopsis fattorussoi sp. nov. (Dinophyceae), a new benthic toxic *Ostreopsis* species from the eastern Mediterranean Sea

Stefano Accoroni,Tiziana Romagnoli,Antonella Penna,Samuela Capellacci,Patrizia Ciminiello,Carmela Dell'Aversano,Luciana Tartaglione,Marie Abboud–Abi Saab,Valentina Giussani,Valentina Asnaghi,Mariachiara Chiantore,Cecilia Totti

Abstract
The new benthic toxic dinoflagellate, *Ostreopsis fattorussoi* sp. nov., is described from the Eastern Mediterranean Sea, Lebanon and Cyprus coasts, and is supported by morphological and molecular data. The plate formula, Po, 3′, 7″, 6c, 7s, 5‴, 2′′′′, is typical for the *Ostreopsis* genus. It differs from all other *Ostreopsis* species in that (i) the curved suture between plates 1′ and 3′ makes them approximately hexagonal, (ii) the 1′ plate lies in the left half of the epitheca and is obliquely orientated leading to a characteristic shape of plate 6″. The round thecal pores are bigger than the other two Mediterranean species (*O*. cf. *ovata* and *O*. cf. *siamensis*). *O. fattorussoi* is among the smallest species of the genus (DV: 60.07 ± 5.63 μm, AP: 25.66 ± 2.97 μm, W: 39.81 ± 5.05 μm) along with *O. ovata*. Phylogenetic analyses based on the LSU and internal transcribed spacer rDNA shows that *O. fattorussoi* belongs to the Atlantic/Mediterranean *Ostreopsis* spp. clade separated from the other *Ostreopsis* species. *Ostreopsis fattorussoi* produces OVTX-a and structural isomers OVTX-d and -e, *O*. cf. *ovata* is the only other species of this genus known to produce these toxins. The Lebanese *O. fattorussoi* did not produce the new palytoxin-like compounds (ovatoxin-i, ovatoxin-j_1, ovatoxin-j_2, and ovatoxin-k) that were previously found in *O. fattorussoi* from Cyprus. The toxin content was in the range of 0.28–0.94 pg · $cell^{-1}$. On the Lebanon coast, *O. fattorussoi* was recorded throughout the year 2015 (temperature range 18°C–31.5°C), with peaks in June and August.

Abbreviations

- **AP**
- anterioposterior diameter
- **DV**
- dorsoventral diameter
- **ITS**
- internal transcribed spacer
- **L:D**
- Light:Dark
- **LC-HR MS^n**
- Liquid Chromatography-High Resolution Multiple Stage Mass Spectrometry
- **ML**
- Maximum Likelihood
- **MP**
- Maximum Parsimony
- **NJ**
- Neighbor Joining
- **OVTX**

- ovatoxin
- **PLTX**
- palytoxins
- **RP**
- resolving power
- **UV**
- Ultraviolet
- **W**
- transdiameter

The genus *Ostreopsis* belongs to the family of Ostreopsidaceae (Gonyaucales, Dinophyceae), which includes two genera of benthic dinoflagellates (i.e., *Ostreopsis* and *Coolia*). The type species, *Ostreopsis siamensis* Schmidt, was first described in the Gulf of Siam (Thailand) in 1900 (Schmidt **1901**). In the following years, several other species have been described by other authors: *O. lenticularis* Fukuyo*, O. ovata* Fukuyo (Fukuyo **1981**), *O. heptagona* Norris, Bomber & Balech (Norris et al. **1985**), *O. mascarenensis* Quod (Quod **1994**), *O. labens* Faust & Morton (Faust and Morton **1995**), *O. marina* Faust, *O. belizeana* Faust and *O. caribbeana* Faust (Faust **1999**, Hoppenrath et al. **2014**). Of late, however, the validity of some *Ostreopsis* species has been questioned. Although the taxonomy of *Ostreopsis* is based on morphological characters (thecal plate pattern, shape and size), high morphological variability is reported within the same species and the original descriptive characters of some species are often considered inadequate to discriminate among most *Ostreopsis* species in field samples (Penna et al. **2005**, Parsons et al. **2012**, David et al. **2013**). In addition to the confusion on the morphological features, no genetic data were provided in these original descriptions and the submission of any further new species description accompanied by a sequence and comparison with other sequences in GenBank has been recommended (Parsons et al. **2012**). Lately, several phylogenetic studies based on LSU and internal transcribed spacer (ITS) analyses have been carried out on *Ostreopsis* species, supplying an increasing number of molecular clades (and subclades) that may represent cryptic species (Penna et al. **2010**, **2014**, Sato et al. **2011**, Tawong et al. **2014**).
Ostreopsis species were reported since a long time in tropical ciguatera endemic areas (Carlson and Tindall **1985**, Bomber and Aikman **1989**) and were often wrongly implicated in incidences of ciguateric syndrome (e.g., Tosteson **1995**). Indeed, some *Ostreopsis* species are toxic, but their toxins (mostly belonging to the palytoxin group) are not those that cause ciguatera. Among the nine species of the genus *Ostreopsis*, toxicity has been demonstrated in *O. siamensis* (also for *O.* cf. *siamensis*), *O. mascarenensis*, *O. lenticularis* and *O.* cf. *ovata* (Nakajima et al. **1981**, Yasumoto et al. **1987**, Holmes et al. **1988**, Mercado et al. **1994**, Meunier et al. **1997**, Lenoir et al. **2004**, Ciminiello et al. **2006**, Scalco et al. **2012**, Uchida et al. **2013**, García-Altares et al. **2015**, Brissard et al. **2015**).
Moreover, *O. heptagona* was determined to be toxic, as methanol extracts of this species isolated from Knight Key (Florida) were weakly toxic to mice (Babinchak, according to Norris et al. **1985**).
In the past decade, *Ostreopsis* blooms have also become common in temperate areas during the summer-autumn period (Chang et al. **2000**, Rhodes et al. **2000**, Pearce et al. **2001**, Vila et al. **2001**, Taniyama et al. **2003**, Turki **2005**, Aligizaki and Nikolaidis **2006**, Mangialajo et al. **2008**, Shears and Ross **2009**, Totti et al. **2010**, Illoul et al. **2012**, Ismael and Halim **2012**, Pfannkuchen et al. **2012**, Selina et al. **2014**). In these areas, *Ostreopsis* blooms are often associated with noxious effects on the health of humans (Tichadou et al. **2010**, Del Favero et al. **2012**) and benthic marine organisms (Accoroni et al. **2011**, Pagliara and Caroppo **2012**, Gorbi et al. **2013**, Carella et al. **2015**).
In the Mediterranean Sea, two genotypes corresponding to the morphotypes *O.* cf. *ovata* and *O.* cf. *siamensis* have been recorded to date (Penna et al. **2010**, **2012**). Almost all knowledge about the ecology of *Ostreopsis* species in the Mediterranean Sea mainly refers to *O.* cf. *ovata* due to its dominance over the other species in this area (Battocchi et al. **2010**, Perini et al. **2011**). Several environmental parameters have been recognized to strongly influence bloom dynamics, such as hydrodynamics, water temperature and nutrients (Vila et al. **2001**, Shears and Ross **2009**, Totti et al. **2010**, Mabrouk et al. **2011**, Mangialajo et al. **2011**, Cohu et al. **2013**).

The genotype *O*. cf. *siamensis* has been detected along the Catalan coast, in the eastern Atlantic coast of Morocco, Portugal, northern Spain and southern Italy (Vila et al. **2001**, Amorim et al. **2010**, Bennouna et al. **2010**, Laza-Martinez et al. **2011**, Ciminiello et al. **2013**, David et al. **2013**) and its morphotype has also been reported along the Tunisian and Lebanese coasts (Turki **2005**, Turki et al. **2006**, Mabrouk et al. **2011**, **2012**, Abboud-Abi Saab et al. **2013**). In addition to these two species, recently Penna et al. (**2012**) found a new genotype probably corresponding to a new species of *Ostreopsis*, in both the Atlantic Ocean (Canary Islands) and Mediterranean Sea (Greece and Cyprus Island). Strains of this new genotype collected in Cyprus have been reported to produce OVTX-a, -d, -e, and isobaric palytoxin, so far found only in *O*. cf. *ovata*, adding three new palytoxin-like compounds to those already identified, i.e., OVTX-i, OVTX-j_1, OVTX-j_2, and OVTX-k (Tartaglione et al. **2016**). This genotype will be described here as a new species. Descriptions of new species are often based on culture material rather than field samples (e.g., Litaker et al. **2009**, Tillmann et al. **2009**, Fraga et al. **2011**, Percopo et al. **2013**, Fraga and Rodríguez **2014**). This approach, however, can have drawbacks when cells in culture strongly change their morphology producing aberrant cells and/or modifying the shape and the size of the thecal plates and the entire cell, as occurs in *Ostreopsis* (Aligizaki and Nikolaidis **2006**, Laza-Martinez et al. **2011**, Nascimento et al. **2012**, Scalco et al. **2012**, David et al. **2013**). Moreover, under certain culture conditions, in addition to the typical vegetative morphology, different stages of life cycle (characterized by different size, shape, and plate tabulation) may appear (Aligizaki and Nikolaidis **2006**, Bravo et al. **2012**, Accoroni et al. **2014**). On the other hand, the observation of culture material is necessary to obtain genetic material for gene sequencing and may be necessary to describe the whole range of morphological variability of a species and its different life stages in order to avoid diverse life stages of the same species being described as different species (Coats **2002**). It is, therefore, crucial to use both culture and natural samples in the description of a new species.

In this study, we describe *Ostreopsis fattorussoi*, a new toxic benthic dinoflagellate found in the Lebanon and Cyprus coasts (Eastern Mediterranean Sea), on the basis of molecular and ultrastructural features of both natural and culture samples. We also investigated the ecology of this new species along the Lebanon coast and analyzed its toxin content and profile.

Materials and Methods

Sampling and sample treatment

Macroalgal samples were collected at three sites from Cyprus and Lebanon in 2013 and 2015, respectively: site 1, Vassiliko Bay, southern coast of Cyprus (34°43′ 19.61″ N, 33°18′ 6.67″ E), site 2, Batroun, Lebanon (34°15′ 5.40″ N, 35°39′ 24.78″ E), and site 3, Byblos, Lebanon (34°06′ 51.84″ N, 35°38′ 53.76″ E; Fig. **1**). All sites were located in shallow and rocky shores.

Macroalgae (mainly *Halopteris scoparia* (Linnaeus) Sauvageau in Cyprus and *Corallina elongata* Ellis & Solander in Lebanon) were sampled and then processed to detach epiphytic cells (see below). Samples for microscope observations were fixed with 0.8% neutralized formaldehyde (Throndsen **1978**) and stored at 4°C in the dark until the analyses.

At site 2 (Batroun, Lebanon), an ecological study about the temporal trend of *Ostreopsis* abundances and the relationships with some environmental parameters was carried out. This site is characterized by a rocky bottom and is affected by the discharge of phosphate into the sea from a chemical factory.

The sampling was carried out monthly from January to April 2015, then every 3–7 d until October 2015. The temperature was recorded using an alcohol thermometer (precision ± 0.1°C). Salinity was measured using an induction salinometer (Beckman RS7-C) once back in laboratory. Surface water samples for nutrient analyses were collected through plastic bottles. Samples were immediately stored at −20°C. Orthophosphates (P-PO_4) were analyzed according to Murphy and Riley (**1962**), nitrites (N-NO_2) and nitrates (N-NO_3) to Strickland and Parsons (**1968**).

Macrophytes and seawater samples were collected in triplicate following the protocol of the ENPI-CBCMED project M3-HABs (**http://m3-habs.net**). Water samples were collected in plastic bottles (250 mL) at 20 cm depth (30 cm above the macroalgae), before the collection of the benthic substrata, in order to avoid resuspension. Portions of macroalgal thalli (~15 g) were collected using 250 mL plastic bottles. Seaweed samples in the storage water were shaken vigorously to dislodge the epiphytic cells, then the thalli were re-

rinsed with filtered seawater to completely remove *Ostreopsis* cells. Finally, the samples were fixed by adding Lugol's solution at 1% V/V and stored at 4°C in the dark until the analyses.

Light microscope analysis

Light microscopy observations for the new species description were carried out using an inverted microscope (Zeiss Axiovert 135, Carl Zeiss, Oberkochen, Germany) equipped with phase contrast, differential interference contrast and epifluorescence with a UV lamp. Field samples were analyzed after staining with the DNA-specific dye SYBR Green to visualize the nucleus and the cellulose specific dye Calcofluor-White M2R to elucidate the thecal morphology.

Microphotographs were taken with a Canon EOS 6D (Canon Inc., Tokyo, Japan) digital camera. In the event that the field depth was not enough for the whole subject, multiple images taken at different focus distances were merged using image manipulation software.

Ostreopsis cells from field samples were measured at 400× magnification using a micrometric ocular. In samples of both Cyprus and Lebanon, 141 cells were measured along the dorsoventral diameter (DV) and the transdiameter (W); for a subset of cells (101) the anterioposterior diameter (AP) was also measured, using a needle to turn them over.

Abundances of *Ostreopsis* cells at site 2 were estimated both in benthic and in planktonic subsamples (1 and 50 mL, respectively) after homogenization. Counting was carried out in Utermöhl chambers (Edler and Elbrachter **2010**) for seawater samples or Sedgewick-Rafter chambers (Guillard **1978**) for benthic samples, through an inverted light microscope (Wild M40, Wild Heerbrugg AG, Heerbrugg, Switzerland) and a light microscope (Motic BA 400, MoticEurope S.L.U., Barcelona, Spain) respectively, both equipped with phase contrast, at 200× magnification. Counting was performed on random transects, or on the half chamber, in order to count a representative cell number. Cell abundances were expressed as cells · g^{-1} fw and cells · L^{-1} for water column.

Estimates of the net growth rates (μ · d^{-1}) of the natural populations of *Ostreopsis* throughout the year were calculated according to:

$$\mu = (\ln N_2 - \ln N_1)/(t_2 - t_1)$$

where N_2 and N_1 are *Ostreopsis* abundances on each benthic substrata at respective sampling day, t_1, or t_2. The abundances of *Ostreopsis* in benthic samples were tested for significant correlations (Pearson) with all recorded environmental parameters and with abundance in the water column. Growth rates were tested for significant correlations (Pearson) with all environmental parameters. The statistical analyses were conducted using Statistica (Statsoft) software.

Scanning electron microscope analysis

Some preserved subsamples (1–5 mL) were dehydrated by immersion in ethanol at increasing gradations (10%, 30%, 50%, 70%, 80%, 90%, 95%, and 100%). After 1 d in absolute ethanol, the dehydrated samples were filtered on a Nucleopore polycarbonate filter, and treated in a Critical Point Dryer (Polaron CPD 7501, Quorum Technologies, Newhaven, UK). Filters were placed on stubs and sputtered with gold-palladium in a Sputter Coater (Polaron SC 7640) for observation under the scanning electron microscopy (FE-SEM; Zeiss Supra 40).

Strain isolation

Ostreopsis cell isolates were obtained from microphytobenthos epiphytic on seaweeds collected on July 2013 and June 2014 at site 1, Vasiliko Bay (Cyprus), and site 2, Batroun (Lebanon), respectively, using the capillary pipette method (Hoshaw and Rosowski **1973**). After an initial growth in microplates, cells were cultured at 23°C ± 1°C under a 14:10 L:D photoperiod and an irradiance of 100 μmol photons · m^{-2} · s^{-1}, in modified f/10 medium Si free (Guillard **1975**) using filtered and autoclaved natural seawater (salinity 35). One (C1005) and five (L1000, L1007, L1008, L1020, and L1022) strains of *Ostreopsis* sp. were isolated from site 1 and 2, respectively (Table **1**).

DNA extraction, PCR amplification, sequence alignment

Genomic DNA was extracted and purified from 50 mL monoclonal cultures of *Ostreopsis* sp. in logarithmic growth phase using a DNeasy Plant Kit (Qiagen, Valencia, CA, USA) according to the manufacturer's instructions. Briefly, cultures were collected by centrifugation at 3,000*g* for 20 min. The supernatant was

removed and the pellets were transferred to a 1.5-mL tube, centrifuged at 13,000*g* for 10 min. The pellets were immediately processed or stored at −80°C until DNA extraction.
The PCR amplification of ribosomal 5.8S gene and non-coding ITS regions, and partial nuclear LSU (D1/D2 domains) were described in Penna et al. (**2010**). Amplified PCR fragments were purified (Penna et al. **2014**) and sent to Eurofins Genomics (Ebersberg, Germany). All nucleotide sequences of ITS-5.8S rDNA and LSU deposited in ENA-EMBL are listed in Table **1**.

Phylogenetic analyses

The ITS-5.8S and LSU sequences were aligned using MAFFT software. Short aligned sequences and ambiguously aligned positions were excluded from the alignment manually or using Gblocks (**http://molevol.cmima.csic.es/castresana/Gblocks.html**) with default settings.
The jModelTest v.2.1.7 (Darriba et al. **2012**) was used to determine the evolutionary model that best fitted data according to Akaike Information Criterion. For both ITS-5.8S and LSU gene rDNA alignment, the most appropriate evolutionary model was found to be HKY+I+G with a gamma distributed rate of variation among sites equal to 1.56 and 1.47, respectively.
Neighbor-Joining (NJ) and Maximum Parsimony (MP) analyses were performed using MEGA6 (Tamura et al. **2013**). The MP analyses were performed using the Tree-Bisection-Redrafting algorithm with search level 1 in which the initial trees were obtained by the random addition of sequences (10 replicates). All positions containing gaps and missing data were eliminated. The robustness of NJ and MP trees was tested by bootstrapping using 1,000 pseudo-replicates. Maximum likelihood (ML) analyses were run with Phyml v.3.0 (Guindon et al. **2010**). Bootstrap values were calculated with 1,000 pseudo-replicates.
Bayesian analyses (BI) were performed using MrBayes v. 3.2.3 (Ronquist and Huelsenbeck **2003**) with the following settings: four Markov chains were run for 2,000,000 generations with a sampling frequency of 100 generations. Log-likelihood values for sampled trees were stabilized after almost 200,000 generations. The last 18,000 trees were used to estimate Bayesian posterior probabilities, whereas the first 2001 were discarded as burn-in. Results from two-independent runs were used to construct a majority-rule consensus tree containing the posterior probabilities.
The sequences of *Coolia monotis* VGO783 (**FN256433**) and VGO786 (**AM902737**) were used as outgroups for the *Ostreopsis* ITS-5.8S and LSU gene phylogenetic analyses, respectively.

Toxin analysis

Reagents for chemical analyses

All organic solvents and water (HPLC grade) and glacial acetic acid (Laboratory grade) were by Sigma Aldrich (Steinheim, Germany). A palytoxin standard (100 µg; lot **LAM7122**) from Wako Chemicals GmbH (Neuss, Germany) was dissolved in methanol/water (1:1, v/v) and used for quantitative analyses. It should be noted that this standard was not certified and may have contained some contaminants other than the palytoxin and that the quali-quantitative composition of this standard can vary between lots. The standard used here contained 83% of palytoxin itself, 5% of 42- hydroxypalytoxin, and 12% of contaminant(s). A crude extract of Ligurian *O*. cf. *ovata* (CBA-29, Giussani et al. **2015**) containing a pool of OVTXs was used as a reference sample for identification of OVTXs in algal extracts.

Toxin extraction

Cell pellets of five *Ostreopsis* strains collected along Lebanon coasts, namely L1002 (8.0×10^6 cells), L1007 (1.0×10^7 cells), L1008 (3.0×10^6 cells), L1020 (4.8×10^6 cells), L1022 (1.0×10^6 cells) were extracted once by adding 1–10 mL of methanol/water (1:1, v/v) to achieve a concentration of around 1.0×10^6 cells · mL^{-1} of extracting solvent. The mixtures were sonicated for 10 min in pulse mode, while cooling in ice bath, and centrifuged at 3,000*g* for 1 min; the obtained supernatants were then decanted and analyzed by LC-HRMS (5 µL injected).

Liquid chromatography-high resolution multiple stage mass spectrometry

MS experiments (positive ions) were carried out on a Dionex Ultimate 3000 quaternary system coupled to a hybrid linear ion trap LTQ Orbitrap XL™ Fourier Transform MS (FTMS) equipped with an ESI ION MAX™ source (Thermo-Fisher, San Josè, CA, USA). A Poroshell 120 EC-C18, 2.7 µm, 2.1 × 100 mm column (Agilent Technologies, Santa Clara, CA, USA) maintained at room temperature was used. It was eluted at 0.2 mL · min^{-1} with water (eluent A) and 95% acetonitrile/water (eluent B), both containing 30 mM acetic

acid. A slow gradient elution was used: 28%–29% B over 5 min; 29%–30% B over 10 min; 30%–100% B over 1 min, and held for 5 min (Ciminiello et al. **2015**).
HR full scan MS experiments (positive ions) were acquired in the range *m/z* 800–1400 at a RP of 60,000 (FWHM at *m/z* 400). The following source settings were used: a spray voltage of 4.8 kV, a capillary temperature of 290°C, a capillary voltage of 17 V, a sheath gas and an auxiliary gas flow of 32 and 4 (arbitrary units). The tube lens voltage was set at 145 V. HR collision induced dissociation MS^2 experiments were acquired at a RP = 60,000 using a collision energy = 35%, isolation width = 3.0 Da, activation Q = 0.250, and activation time = 30 ms. The most intense peak of the $[M+H+Ca]^{3+}$ ion cluster of OVTX-a (*m/z* 896.1) and OVTX-d/-e (*m/z* 901.4) were used as precursors in $HRMS^2$ experiments. Calculation of elemental formulae was performed using the mono-isotopic peak of each ion cluster using Xcalibur software v. 2.0.7 with a mass tolerance constrain of 5 ppm. The isotopic pattern of each ion cluster was taken into account in assigning molecular formulae. Extracted ion chromatograms of the detected OVTXs were obtained by selecting the $[M+H+Ca]^{3+}$ ion clusters, using a mass tolerance of 5 ppm and employed in quantitative analyses. Due to availability of the only palytoxin standard, quantitative determination of OVTX-a, -d, and -e in the extracts was carried out by using a calibration curve (triplicate injection) of palytoxin standard at seven concentrations (1,000, 500, 250, 125, 62.5, 31.2, and 15.6 ng · mL^{-1}). OVTX molar responses were assumed to be similar to that of PLTX. Calibration curve equation was $y = 2{,}455.6x - 19{,}184$ and its linearity was expressed by $R^2 = 0.9976$. The limit of detection for palytoxin in pure solvent was 13 ng · mL^{-1} after correction for the 83% purity of the standard.

Results

Ostreopsis fattorussoi Accoroni, Romagnoli et Totti **sp. nov.**
Diagnosis. Cells are ovate in shape and ventrally pointed with a DV of 42.5–72.5 µm, AP of 20–32.5 µm and W 26.3–50 µm. The thecal plate formula is Po, 3', 7", 6c, 7s, 5"', 2''''. Thecal plates are smooth with evenly distributed same-sized round pores. The apex is strongly eccentric, located on the left dorsal side of the epitheca. The apical pore plate Po is 10–12.5 µm long and slightly curved. Plate 1' is heptagonal, oblique, and is almost entirely in the left half of the epitheca. Plate 3' is hexagonal, almost entirely in the left half of the epitheca. The pentagonal 6" has the 6"/5" suture length almost twice as long as the 6"/7" suture length. The narrow sulcal groove runs obliquely from the left side of the ventral area into the hypotheca. Cells are photosynthetic. The nucleus has a slightly elongated (subspherical) shape positioned obliquely and occupies the dorsal part of the cell. The species is toxic producing ovatoxins.
Holotype: SEM stub n. 3/16-UNIVPM deposited at the Botanical Museum of the Università Politecnica delle Marche, Ancona Italy, in the Herbarium Anconitanum (ANC). Figure 5A represents the holotype.
Isotype. Preserved sample, deposited at the Università Politecnica delle Marche, Ancona Italy, in the Herbarium Anconitanum (ANC).
Preserved DNA of clonal strain CBA-L1020, barcoded in ENA-EMBL (EMBL ID: LT220224), held at the Dipartimento di Scienze Biomolecolari, Università di Urbino, Italy.
Type Locality. Batroun, Lebanon (34°15' 5.40" N, 35°39' 24.78" E, Fig. **1**).
Habitat. Benthic, often epiphytic on seaweeds or living on other substrata; it was shown that it could also be resuspended into the water column.
Etymology. The specific epithet honors our dear colleague Prof. Ernesto Fattorusso from the University of Napoli Federico II, who significantly contributed to the study of algal biotoxin structures and elucidation of novel organic metabolites produced by marine algae.
Distribution: Eastern Mediterranean (i.e., Cyprus, Lebanon coasts). The same genotype is known also in Crete (David et al. **2013**, Penna et al. **2014**), Canary Islands, Spain (Penna et al. **2010**) and Puerto Rico, USA (David et al. **2013**).

Morphology

Cells are ovate and ventrally slender with average DV 60.1 ± 5.6 (42.5–72.5) µm, AP 25.7 ± 3 (20–32.5) µm, and W 39.8 ± 5.1 (26.3–50) µm. The DV:AP ratio is 2.35 ± 0.22, while DV:W is 1.52 ± 0.14.
The thecal plate formula is Po, 3', 7", 6c, 7s, 5"', 2'''' (Figs. **2** and **3**). Thecal plates are smooth with evenly distributed round pores visible using LM with Calcofluor-White M2R staining (Fig. **4**A). Small perforations are located inside the pores (Fig. **5**E). They are scattered on the epi- and hypothecal plates and lined up along the border of the pre- and postcingular plates close to the cingular groove (Fig. **5**, A and B) and the

borders of the two cingular lists (Fig. 5D). Only one size class pore is visible ranging from 0.26 to 0.53 µm (0.38 ± 0.08 µm) with 11–15 pores per 100 µm^2. Cells produce extracellular mucilage and a complex network of filaments is extruded through the thecal pores (Fig. 6D).

Both epitheca and hypotheca are equal in size. The apex is strongly eccentric, located on the left dorsal side of the epitheca. The apical pore plate Po is 11.67 ± 1.44 µm long, slight curved and contacts the three apical plates. Plate 1′ is heptagonal and almost entirely lies in the left half of the epitheca and is not parallel to the dorsoventral axis, but its dorsal part is shifted on the left and dorsally pointed. Plate 1′ touches plates 2′, 3′, 1″, 2″, 6″, and 7″. Plate 2′ is narrow and almost twice the size of Po, separating the 3′ and 3″ plates. Plate 3′ is hexagonal, almost entirely located in the left half of the epitheca, and it is dorsally displaced.
Among the seven irregularly quadrangular (with the only exception of the plate 6″) precingular plates 1″, and 4″ are the smallest. Because of the left and dorsal displacement of 3′, plate 5″ is transversally elongated and 3″ appears as narrow and dorsally elongated as plate 2″ (Figs. 4, A and C; 5A). The characteristic shape of the pentagonal 6″ is due to the oblique orientation of the 1′ and the 6″/5″ suture length is almost twice as long as 6″/7″ suture length, resulting in an oblique 6″/1′ suture; moreover, its length:width ratio is 1.06 ± 0.11 (0.94–1.2) and the 3′/6″ suture is dorsally shifted. The first and the last precingular plates (i.e., 1″ and 7″, respectively) are extended and elongated, tapering toward the sulcal area. Plate 2″ is narrow and the 4″ has a similar size of 3′.
The cingulum is descending and displaced one time its width and consists of six plates, almost of the same length.
The narrow sulcal groove runs obliquely from the left side of the ventral area into the hypotheca. The ventral side of the 1‴ plate forms a “wing” that covers almost all the sulcal area of the hypotheca (Fig. 4, D–F) leading well identifiable only 5 plates in intact cells (Fig. 6A): the anterior sulcal plate (Sa), the left anterior sulcal plate (Ssa), the right-anterior sulcal plate (Sda), the right-posterior sulcal plate (Sdp), and the posterior sulcal plate (Sp). In broken cells, a further two plates are identifiable on the inner left side of the sulcus: the left posterior sulcal plate (Ssp) and the accessory anterior sulcal plate (S.ac.a.) (Fig. 6, B and C).
In the upper part of the ventral area, a conspicuous tube-like structure, the ventral tube (Vt), ends with the ventral opening (Vo, Figs. 4D and 6, A and B). The upper half of the Vt is surrounded by the small Sa and the lower half by the elongated Ssa. The Sa is small and touches the ventral part of the 1″ and 7″ plates. The Ssa plate is wide and extends from the lower side of the Sa and Vt to the first cingular plate (C1) and the S.ac.a. plate. The left (i.e., the anterior) margin of the Ssa plate touches the 1″ plate, while the right (i.e., the posterior) margin is in contact with the anterior, sigmoid edge of the Sda plate.
The Sda plate is the most elongated of all the sulcal plates. Its anterior part is curved toward the epitheca and contacts, from right to left, the sixth cingular (C6), the 7″ and the Sa plates. It surrounds the right (i.e., the posterior) margin of plate Ssa along its whole side. The left portion of the Sda plate is hidden by the 1‴ and contacts the Ssp plate in the bottom of the sulcal groove. At its posterior part, Sda contacts the ventral end of the 5‴ and the narrow Sdp.
In the end of the sulcal groove, the right-anterior part of the irregularly triangular Sp touches the ventral end of the 5‴ plate, and its right-posterior part adjoins to a small portion of the ventral end of the 2‴ plate (Fig. 4E) The upper part of the Sp connects with the Sdp and in its posterior part to the Ssp.
The other side of the sulcal groove (and therefore completely covered by the 1‴ plate) consists of the almost quadrangular S.ac.a. plate for the small upper part (Fig. 6C) and the elongated Ssp makes up rest of the groove.
Among the five postingular plates, the triangular 1‴ plate is the smallest of the series. The 2‴ plate is wide and quadrangular. The quadrangular 3‴ and 4‴ plates occupy most of the dorsal part of the hypotheca, while the 5‴ plate is oblong and quadrangular, although the ventral side is very short. There are two antapical plates which are both pentagonal. The 1‴ plate is much smaller than the 2‴ plate which occupies the center of the hypotheca (Figs. 4, E and F; 5B).
There are numerous elongated chloroplasts located within the cell periphery. The nucleus, has a slightly elongated (often subspherical) shape (13.6 ± 2.0 µm long, 8.8 ± 1.7 µm wide) positioned obliquely in the dorsal part (from the right to the center) of the cell (Fig. 4B).

Phylogenetic analyses of *Ostreopsis* ITS-5.8S and LSU ribosomal genes

The final alignments of *Ostreopsis* spp. ribosomal gene sequences, as ITS-5.8S and LSU with *Coolia monotis* VGO783 and VGO786 as outgroups, respectively, were as follows: ITS-5.8S was 419 bp in length (A = 27%, T = 34.8%, C = 18.2%, G = 20%) with 116 polymorphic sites, of which 93 parsimony informative, and a transition/transversion ratio of 1.7; LSU was 701 bp in length (A = 28.5%, T = 32.9%, C = 16.9%, G = 21.7%) with 343 polymorphic sites, of which 284 parsimony sites, and a transition/transversion ratio of 1.4.

Based on single ITS-5.8S and LSU rDNA sequences, only minor differences between the NJ, MP, ML and Bayesian inference analyses were found; therefore, only the ML phylogenetic trees are presented (Figs. 7 and 8). The ITS-5.8S rDNA phylogeny, based on 46 isolates of *Ostreopsis* spp., identified three major clades within the genus *Ostreopsis*: the first comprising *Ostreopsis* sp. CBA0203 from Hawaii, and strains identified as *O*. cf. *lenticularis*, *O*. cf. *labens* and *Ostreopsis* sp. 6 (Tawong et al. **2014**) from Pacific Ocean; the second clade comprised the *O*. cf. *siamensis*, and *Ostreopsis* sp. (now identified as *O. fattorussoi*) from eastern Mediterranean Sea, Greece (KC84, KC86, Penna et al. **2014** and Dn83EHU, David et al. **2013**), Lebanon and Cyprus (this study), with *Ostreopsis* sp. VGO881 (Canary Islands) and *Ostreopsis* sp. Dn110EHU (Porto Rico) from Atlantic Ocean. Finally, the third grouping included *O*. cf. *ovata* complex from Atlantic, Mediterranean, and Pacific. All these clusters were supported by high bootstrap and posterior probability values.

The LSU rDNA phylogeny that was obtained from 40 isolates of *Ostreopsis* spp. showed some differences in tree topology compared with ITS-5.8S rDNA phylogenetic analysis. The first splitting clade from outgroup *Coolia* included two sub-clades of *O*. cf. *lenticularis* and *Ostreopsis* sp. along with *Ostreopsis* sp. 5 and *Ostreopsis* sp. CBA0203; all these isolates derived from Indian and Pacific Ocean. The second clade grouped the *Ostreopsis* sp. (now identified as *O. fattorussoi*) from eastern Mediterranean Sea (Lebanon, Greece and Cyprus) and Atlantic VGO881 isolate. The third clade comprised all *O*. cf. *ovata* isolates collected from many sites worldwide and *O*. cf. *siamensis*. All these lineages were strongly supported by high bootstrap and posterior probability values.

The difference of base pairs between *O. fatturossoi* and other *Ostreopsis* species ranged from 200 to 231 bp, and from 99 to 82 bp based on LSU and ITS-5.8S rDNA analysis of net nucleotide average difference, respectively.

Temporal trend and relationships with environmental parameters

Ostreopsis cells were detected at the Batroun site throughout the year with two blooming periods, the first observed between the end of May and the beginning of July and the second in August (Fig. 9B). Maximum abundances were detected on 2 July 2015 (28×10^3 cells $\cdot$ g^{-1} fw) and on 22 June 2015 (840 cells $\cdot$ L^{-1}) on benthic substrata and in the water column, respectively.

The correlation between *Ostreopsis* abundances on benthic substrata and those in the water column was positive and significant ($n = 9$; $r = 0.79$; $P < 0.05$).

Surface temperature ranged from 18°C to 31.5°C with maximum temperatures of 29.5°C to 31.5°C occurring from the end of July to early October and minimum values of around 18°C in the first months of the year. The maximum values of *Ostreopsis* abundances were recorded when water temperature ranged from 27°C to 29.7°C (Fig. 9B). Throughout the year, the salinity ranged from 38.14 to 39.43. Correlation analyses among *Ostreopsis* abundances, growth rate, temperature, and salinity revealed no significant relationships.

No obvious trends were determined for of NO_2, NO_3 and PO_4 (Fig. 9A). Only NO_3 showed high values (>1.3 µmol $\cdot$ L^{-1}) in January and February compared with the rest of the year, when values ranged from 0.156 to 0.626 µmol $\cdot$ L^{-1}. NO_2 concentrations were markedly lower than those of nitrates, ranging from 0.015 to 0.250 µmol $\cdot$ L^{-1}. No significant relationships were found between *Ostreopsis* abundances (or growth rate) and both NO_2 and NO_3. PO_4 concentrations ranged from 0.015 to 0.433 µmol $\cdot$ L^{-1} and rarely exceeded 0.150 µmol $\cdot$ L^{-1} throughout the year. The two maximum values of PO_4^{3-}, i.e., 0.433 and 0.175 µmol $\cdot$ L^{-1}, were recorded in February and June, respectively. Although no correlation

between *Ostreopsis* abundances and PO_4 concentrations was detected, a positive and significant correlation was found between *Ostreopsis* growth rates and PO_4 concentrations (n = 9; r = 0.87; P < 0.01).

Toxicity

Crude extracts of five strains of *O. fattorussoi* collected along the Lebanese coast (i.e., L1002, L1007, L1008, L1020, and L1022) were analyzed by LC-HRMS^n (n = 1, 2) to characterize their toxin profiles and measure their toxin content. The analyses were carried out with a palytoxin standard and a Ligurian *O.* cf. *ovata* extract containing OVTX-a, -d and –e and isobaric palytoxin (Giussani et al. **2015**). The chromatographic conditions allowed the separation of all of the analogs contained in the extracts.
Toxin extracts from the five Lebanese strain of *O. fattorussoi* revealed three strains to be toxic; L1007, L1020, and L1022 all contained OVTX-a, -d, and -e. Their identity was ascertained based on comparison of their retention times and associated full MS spectra (Fig. 10) with those of OVTX-a, -d, -e, contained in the reference extract. Further confirmation for the identity of OVTX-a and of the structural isomers OVTX-d and -e was provided by their LC-HRMS^2 spectra.
Extracts L1002 and L1008 did not contain any palytoxin congener. Considering the extraction volume, the presence of toxins in pellet (1×10^6 cells), could be excluded at levels ≤15 fg · cell^{-1}.
The results of the quantitative analysis are shown in Table 2.

Discussion

In the Mediterranean Sea, only two *Ostreopsis* species have been recorded until now, *O.* cf. *ovata* and *O.* cf. *siamensis* (Vila et al. **2001**, Penna et al. **2005**, **2010**, Battocchi et al. **2010**, Totti et al. **2010**, Mangialajo et al. **2011**, Perini et al. **2011**, Mabrouk et al. **2012**, Abboud-Abi Saab et al. **2013**, Accoroni and Totti **2016**). Recently, new molecular phylogenetic analyses based on ribosomal DNA identified another clade (*Ostreopsis* sp.) distinct from *O.* cf. *ovata* and *O.* cf. *siamensis*, in the eastern Atlantic and Mediterranean coasts, particularly from islands of Cyprus and Crete (Penna et al. **2012**, Tartaglione et al. **2016**). In this study, we name and describe this new genotype as a new species of *Ostreopsis*, named *O. fattorussoi*, by analyzing samples from coasts of Lebanon and Cyprus (Mediterranean Sea). In this study, the description of the thecal tabulation and the morphometrical analyses of this new species were performed on field samples only, as cultured specimens of *O. fattorussoi* frequently demonstrated modifications in shape, size and thecal pattern, as already reported in other *Ostreopsis* species (Norris et al. **1985**, Laza-Martinez et al. **2011**, Nascimento et al. **2012**, Scalco et al. **2012**, David et al. **2013**). For example, a cultured Indonesian strain of *O.* cf. *ovata* (CBA-6) has been observed either to show (Parsons et al. **2012**) or not (Penna et al. **2010**) the contact between the 1′ and 5″ plates, which is a defining plate pattern character of *O. heptagona*. The numerous strains of *O. fattorussoi* were used to characterize the toxic profile and to perform the molecular sequencing of this new species.
The plate tabulation of *Ostreopsis* has been frequently reassessed over the years from its first descriptions (Table 3). The first interpretations of the thecal plates were given by Schmidt (**1901**) and later by Fukuyo (**1981**), who included a partial plate formula of Po, 3′, 7″, 4‴ (+ accessory small plates), 1 antapical plate and Po, 3′, 7″, 5‴, 1′′′′, respectively. This plate pattern interpretation based on Kofoidian plate tabulation was adopted by Norris et al. (**1985**) and Faust et al. (**1996**) who, however, labeled the large hypothecal plate at the antapex (i.e., 1′′′′ in Fukuyo (**1981**)) as a posterior intercalary plate (1p). Over the years, several other authors followed this plate pattern interpretation, although often with a little variation (Penna et al. **2005**, Sato et al. **2011**, Kang et al. **2013**, Hoppenrath et al. **2014**).
On the contrary, Besada et al. (**1982**) did not follow the plate pattern suggested by Fukuyo (**1981**) but reinterpreted the apical plate pattern, providing for the first time a complete plate formula (Po, 4′, 6″, 6c, 8s, 5‴, 2′′′′) which was closer to that of gonyaulacoid dinoflagellates. In this view, the epithecal tabulation was strongly rearranged as the plate considered as 1″ (precingular) in Fukuyo (**1981**) and Faust et al. (**1996**) was considered homologous to the first apical plate of the Gonyaulacales and therefore was named 1′. As a consequence, the plate tabulation included four apical and six precingular plates. This interpretation has been re-adopted by Escalera et al. (**2014**) for *Ostreopsis* cf. *ovata* and was applied to *Gambierdiscus* and *Coolia* as well as by other authors (Fraga et al. **2011**, Mohammad-Noor

et al. **2013**, Fraga and Rodríguez **2014**), arguing that, although this interpretation does not follow the strict relationships among the plates, it takes into account their homology, according to the tabulation of Gonyaulacales (Balech **1980**, Fensome et al. **1993**).
In this paper, we adopted the interpretation of the thecal plates used by Hoppenrath et al. (**2014**), who mainly followed the original description of Fukuyo (**1981**), Norris et al. (**1985**) and Faust et al. (**1996**) regarding the epitheca, and Besada et al. (**1982**) regarding the hypotheca, recognizing that there is no an intercalary plate in *Ostreopsis*. In this regard, we observed that the large hypothecal plate at the antapex contacts the Sp plate (and therefore the sulcus), although the contact area is very narrow and not always visible, confirming that is not an intercalary but an antapical plate (i.e., the 2′′′′), as suggested by Hoppenrath et al. (**2014**). The uncertainty in the attribution of the large hypothecal plate (i.e., 1p vs. 1′′′′) may be explained by the contact point of this plate with the sulcus that may not be visible in some species (Hoppenrath et al. **2014**), as also within the same species (Sato et al. **2011**, Escalera et al. **2014**).
Ostreopsis fattorussoi could quickly be distinguished from the other two Mediterranean species in LM by its round thecal pores which are easily visible and appear larger than those in both *O*. cf. *ovata* and *O*. cf. *siamensis* (Table **4**). Moreover, differently from *O*. cf. *ovata*, which shows pores of two size classes (Penna et al. **2005**, Kang et al. **2013**), pores of only one size class were visible in *O. fattorussoi*. Another way to distinguish *O. fattorussoi* from *O*. cf. *ovata* is the Po, which is longer in the former (Table **4**). Moreover, the shape of the 6″ plate is different: the 6″/5″ suture length is almost twice as long as 6″/7″ suture length, and the length:width ratio of the plate 6″ is 1.06 ± 0.11 (0.95–1.2), while in *O*. cf. *siamensis* and *O*. cf. *ovata* is 1.5 ± 0.2 (1.1–2.4) and 1.6 ± 0.2 (1.3–2.1), respectively (David et al. **2013**).
Moreover, *O. fattorussoi* is readily distinguishable from the other *Ostreopsis* species because of some peculiar characteristics of its plate tabulation (Fig. **11**). (i) in *O. fattorussoi* the 1′ plate lies in the left half of the epitheca and is obliquely orientated giving a characteristic shape to the 6″ plate and the oblique 6″/1′ suture. In all other *Ostreopsis* species, the 1′ plate closely occupies the center of the epitheca and is not oblique. (ii) *O. fattorussoi* is readily identifiable by the curved suture between 1′ and 3′ which makes plates 1′ and 3′ approximately hexagonal, while in the other *Ostreopsis* species they are pentagonal (with the exception of *Ostreopsis heptagona* which have a quadrangular 3′ and a heptagonal 1′ plate).
In *O. fattorussoi*, the 2′ plate is narrow and almost twice the size of Po, separating the 3′ and 3″ plates. This characteristic could be useful to distinguish *O fattorussoi* from many of the other *Ostreopsis* species, as only in *O. heptagona* and *O. labens* does plate 2′ seem to divide plate 3′ from plate 3″ (Fig. **11**). This characteristic may also be present in other *Ostreopsis* species but just not reported in their morphological descriptions: for example, in the original description of *O. ovata*, Fukuyo (**1981**) indicated that this plate does not touch the plate 4″, while this contact was indicated later by Besada et al. (**1982**). Similarly, *O*. cf. *ovata* has been described with (Selina and Orlova **2010**, Kang et al. **2013**) or without this contact (Escalera et al. **2014**).
The hypotheca of *O. fattorussoi* does not show differences with that of *O*. cf. *ovata* (see Selina and Orlova **2010**, Hoppenrath et al. **2014**), although it does differ from the original drawings of *O*. *ovata* by Fukuyo (**1981**) (e.g., the latter has smaller 1′′′′ plate, a longer 2′′′′/4′′′ suture, a longer and narrower 2′′′ plate and a smaller 3′′′).
The correct identification of *Ostreopsis* species in field samples based only on morphometric characters is often highly problematic. As the species recorded in Mediterranean Sea until now (*O*. cf. *ovata* and *O*. cf. *siamensis*) are very similar in shape and size, the DV/AP ratio was proposed as a characteristic for a quick distinction between the two species. Originally a DV/AP ratio of <2 for *O*. cf. *ovata* and >4 for *O*. cf. *siamensis* was proposed (Penna et al. **2005**, Aligizaki and Nikolaidis **2006**, Selina and Orlova **2010**). The situation is now slightly more complex giving that *O*. cf. *ovata* from the northern Adriatic Sea was shown to have a DV/AP ratio slightly higher than 2, ~2.3–2.4 (Monti et al. **2007**, Guerrini et al. **2010**, Accoroni et al. **2012b**). *Ostreopsis fattorussoi* has a DV/AP ratio of 2.35 ± 0.22 µm so this character is of no use to discriminate between *O. fattorussoi* and *O*. cf. *ovata*.

Considering cell size, *O. fattorussoi* seems to be on average slightly bigger (DV: 60.1 ± 5.6 µm, AP: 25.7 ± 3 µm, W: 39.8 ± 5.1 µm) than *O*. cf. *ovata*, but these dimensions still fall within the upper range of the morphological variability reported for the latter species in natural samples (e.g., Accoroni et al. **2012b**, Kang et al. **2013**, Carnicer et al. **2015**).

Ostreopsis fattorussoi and *O. ovata* are the smallest species of the genus and misidentification in field samples, in case both were present, is likely. In this regard, David et al. (**2013**) who stated their difficulties in distinguishing on a morphological base *Ostreopsis* spp. in field samples, most likely showed *O. fattorussoi* and certainly not *O*. cf. *ovata* in their Figure 6A, given both the oblique plate 1' and 1'/6" suture and the wide thecal pores and Po. If true then the distribution of *O. fattorussoi* is likely to include the Atlantic section of the Iberian Peninsula.

The ITS-5.8S and D1/D2 LSU ribosomal genes were able to consistently delineate divergences at the species level among *Ostreopsis* species (Sato et al. **2011**, David et al. **2013**, Penna et al. **2014**, Tawong et al. **2014**). In particular, the rDNA phylogeny showed clearly that strains belonging to *O. fattorussoi* were included in a distinct clade; in fact, both ITS-5.8S and LSU rDNA tree topologies were very similar. The phylogenetic inference obtained from rDNA sequences was robust demonstrating that the clade grouping *O. fattorussoi* strains was supported by high values of bootstraps and Bayesian inferences. Specifically, the ITS phylogeny indicated the existence of *O. fattorussoi*, which included strains from eastern Mediterranean and Atlantic, as sister clade of *O*. cf. *siamensis*. The LSU phylogeny also indicated the presence of *O. fatturossoi* as a distinct species. This clade represented the second grouping that segregated from the first one comprising *Ostreopsis* sp., *Ostreopsis* sp. 5, and *O*. cf. *lenticularis*. Furthermore, collectively the rDNA phylogenies indicated the existence of at least other six different species (Sato et al. **2011**, Penna et al. **2014**, Tawong et al. **2014**).

This is the first report of *O. fattorussoi* in Lebanese coastal waters. The same species (reported as *Ostreopsis* sp.) has previously been reported in Cyprus coastal waters by Tartaglione et al. (**2016**). Besides Cyprus and Lebanon, molecular analyses revealed that the same genotype was found in Crete, Canary Islands (Spain) and Puerto Rico (USA) (Penna et al. **2010**, **2014**, David et al. **2013**).

In the coastal waters of Lebanon, records of *Ostreopsis* species date back from 1979 (Abboud-Abi Saab **1989**), and until now, the only reported species was *O. siamensis,* which has been recorded between July and September in the majority of the rocky coasts (Abboud-Abi Saab et al. **2013**). In this study, *Ostreopsis* cells were detected throughout the year at the Lebanese coastal site, differently from the strongly seasonal trends observed in other Mediterranean areas (Accoroni et al. **2016**). Molecular quantitative analysis by qPCR carried out in Lebanese samples indicated that *O. fattorussoi* was the dominant (often exclusive) *Ostreopsis* species, while the presence of *O*. cf. *ovata* was almost negligible (Casabianca S. and Penna A. pers. comm.). Abundances of *O. fattorussoi* were two orders of magnitude lower than those of *O*. cf. *ovata* recorded in other Mediterranean areas during their summer-late summer blooms (e.g., Mangialajo et al. **2011**, Accoroni et al. **2015**). However, it should be noted that in our study, the sampling was carried out mainly on *Corallina elongata*, a red alga with calcified (and therefore heavy) thallus that strongly influences the values of *Ostreopsis* abundances when they are expressed as cells · g^{-1} fw. *Ostreopsis* maximum abundances were detected during the warmest months with two blooming periods in June–July and August. *Ostreopsis* blooms are generally summer events in temperate areas and maximum abundances are normally associated with the highest recorded temperatures (e.g., Aligizaki and Nikolaidis **2006**, Mangialajo et al. **2008**). However, some exceptions have been detected in the northern Adriatic Sea (Monti et al. **2007**, Accoroni et al. **2012a**) and the Sea of Japan (Selina et al. **2014**), where blooms develop and reach maximum abundances at temperature values below the summer maximum. Similarly, *O. fattorussoi* showed the highest abundances when temperature values were between 27°C and 29.7°C, i.e., lower than the summer maximum (31.5°C). This would suggest that other environmental factors besides temperature may affect the development of *Ostreopsis* abundances. Several studies have provided increasing evidence of a link between harmful algal events and the nutrient enrichment of coastal waters (Glibert and Burkholder **2006**, Heisler et al. **2008**, Glibert et al. **2010**). Although a correlation between *O. fattorussoi* abundances and nutrient concentrations was not observed, a significant correlation was highlighted between *O. fattorussoi* growth rates and phosphate concentrations. The link between an influx of phosphorus-rich waters and higher net growth rate of *O*. cf. *ovata* has already been recognized in the northern Adriatic Sea (Accoroni et al. **2015**).

Ostreopsis species have been shown to produce different toxins, mostly belonging to the palytoxin group. Mediterranean *O*. cf. *ovata* strains produce palytoxin analogs, such as isobaric palytoxin, OVTX -a, b, c, d, e, f, g, and h (Ciminiello et al. **2010**, **2012b**, Scalco et al. **2012**, Brissard et al. **2015**, García-Altares et al. **2015**). On the contrary, the Mediterranean *O*. cf. *siamensis* strain was shown relatively non-toxic, producing only sub-fg levels of palytoxin (Ciminiello et al. **2013**).

Blooms of *Ostreopsis* are well known in the Mediterranean Sea due to their effect on human health, mainly following inhalation of seawater droplets containing *Ostreopsis* cells or fragments and/or aerosolized toxins (Gallitelli et al. **2005**, Kermarec et al. **2008**, Tichadou et al. **2010**, Del Favero et al. **2012**, Casabianca et al. **2013**, Ciminiello et al. **2014**). The typical symptoms of *Ostreopsis* intoxication through aerosol and/or direct contact exposure are broncho-constriction, dyspnoea, fever, conjunctivitis, and skin irritations. Moreover, in the Mediterranean Sea, *Ostreopsis* toxins were found to contaminate seafood (Aligizaki et al. **2008**, Ciminiello et al. **2015**, Pelin et al. **2016**). Several laboratory studies have shown that *Ostreopsis* exerts toxicity also on several marine organisms, both invertebrates and vertebrates (Faimali et al. **2012**, Gorbi et al. **2012**, **2013**, Pagliara and Caroppo **2012**, Carella et al. **2015**). So far, no reports of human intoxications have been reported from Lebanon coast (Abboud-Abi Saab, pers. comm).

Recently, Tartaglione et al. (**2016**) described the toxin profile of *Ostreopsis* sp. (named now as *O. fattorussoi*) isolated from Cyprus waters, showing some strains to produce isobaric palytoxin and OVTX-a, d and e, previously found only in *O*. cf. *ovata*, while some others produced only new palytoxin-like compounds named OVTX-i, OVTX-j_1, OVTX-j_2, and OVTX-k. In this study, we showed that two of the five analyzed Lebanese strains of *O. fattorussoi* were not toxic, and three produced OVTX-a and the structural isomers OVTX-d and -e. The confirmation for the identity of these toxins was provided by their perfectly superimposable LC-$HRMS^2$ spectra over those of previously characterized OVTX-a, -d, and -e (Ciminiello et al. **2010**, **2012a**, Dell'Aversano et al. **2015**). The toxin profile of these strains also matched those of other *O. fattorussoi* strains from Cyprus (Tartaglione et al. **2016**) and those found in ~40% of the Mediterranean *O*. cf. *ovata* strains analyzed so far (Dell'Aversano et al. **2015**). However, Lebanese *O. fattorussoi* strains analyzed here did not produce any new palytoxin-like compounds such as those found in Cypriot *O. fattorussoi* (OVTX-i, OVTX-j_1, OVTX-j_2, and OVTX-k, Tartaglione et al. **2016**).

So far, the toxin content of *O. fattorussoi* strains has occurred in the range of 0.06–2.8 pg · $cell^{-1}$ (Cyprus strains, Tartaglione et al. **2016** and Lebanese strains, this study) which is significantly lower than that of the Mediterranean *O*. cf. *ovata* strains maintained in the same cultured conditions (up to 44.0 pg · $cell^{-1}$, Tartaglione et al. **2016**). This has also been further supported by eco-toxicological tests on *Artemia salina* nauplii showing that *O. fattorussoi* from Cyprus had very low toxicity compared to *O*. cf. *ovata* (Tartaglione et al. **2016**).

In conclusion, despite of the difficulties often reported concerning the identification of *Ostreopsis* species based on morphological characters alone (Penna et al. 2005, Parsons et al. 2012, David et al. 2013), *O. fattorussoi* does show some morphological features that lead unequivocally to its identification. These include:

the curved suture between plate 1' and 3' which makes plates them approximately hexagonal.

the 1' plate that lies in the left half of the epitheca and is obliquely orientated

the characteristic shape of plate 6": its length:width ratio of 1.06 ± 0.11 (0.95–1.2) and the 6"/5" suture length is almost twice as long as that of 6"/7'.

Moreover, the phylogenetic analyses show that *O. fattorussoi* belongs to the Atlantic/Mediterranean *Ostreopsis* spp. clade distinct from the other *Ostreopsis* species.

This benthic dinoflagellate has been detected along the Lebanon coast throughout the year 2015 (with temperatures ranging from 18°C to 31.5°C), with bloom occurring in June and August and a significant correlation was highlighted between *Ostreopsis* growth rates and phosphate concentrations.

O. fattorussoi is a toxic species producing OVTX-a and structural isomers OVTX-d and –e, so far found only in *O*. cf. *ovata*, and three exclusive palytoxin-like compounds (OVTX-i, OVTX-j_1, OVTX-j_2, and OVTX-k, Tartaglione et al. **2016**). All the data collected on this new species about its toxicity so far, however, would suggest a lower risk to human health and marine fauna to that of *O*. cf. *ovata*.

We gratefully acknowledge Demetris Kletou for the help in collecting Cyprus samples, Antonia Mazzeo for her assistance with the chemical analysis of toxins and Silvia Casabianca for molecular information about Lebanese *Ostreopsis* occurrence. A special thanks to Neil T.W. Ellwood for the English revision. This

publication has been produced with the financial assistance of the European Union under the ENPI CBC MED Programme (M3-HABs project). The LC-HRMS study was granted by Programme STAR Linea 1 2013 (VALTOX, Napoli_call2013_08) financially supported by UniNA and Compagnia di San Paolo.

Note

- [Correction added on December 2, 2016, after first online publication: page 15, at the end of 3rd paragraph, pentagonal changed to heptagonal].

REFERENCES

Abboud-Abi Saab, M. 1989. Les Dinoflagellés des eaux côtières libanaises. Espèces rares ou nouvelles du phytoplancton marin. *Leb. Sci. Bull.* **5**: 5– 16.
Google Scholar
Abboud-Abi Saab, M., Fakhri, M., Kassab, M. T. & Matar, N. 2013. Seasonal and spatial variations of the dinoflagellate *Ostreopsis siamensis* in the Lebanese coastal waters (Eastern Mediterranean). *Cryptogamie Algol.* **34**: 57– 67.
CrossrefGoogle Scholar
Accoroni, S., Colombo, F., Pichierri, S., Romagnoli, T., Marini, M., Battocchi, C., Penna, A. & Totti, C. 2012a. Ecology of *Ostreopsis* cf. *ovata* blooms in the northwestern Adriatic Sea. *Cryptogamie Algol.* **33**: 191– 8.
CrossrefGoogle Scholar
Accoroni, S., Glibert, P. M., Pichierri, S., Romagnoli, T., Marini, M. & Totti, C. 2015. A conceptual model of annual *Ostreopsis* cf. *ovata* blooms in the northern Adriatic Sea based on the synergic effects of hydrodynamics, temperature, and the N: P ratio of water column nutrients. *Harmful Algae* **45**: 14– 25.
CrossrefCASWeb of Science®Google Scholar
Accoroni, S., Romagnoli, T., Colombo, F., Pennesi, C., Di Camillo, C. G., Marini, M., Battocchi, C. et al. 2011. *Ostreopsis* cf. *ovata* bloom in the northern Adriatic Sea during summer 2009: ecology, molecular characterization and toxin profile. *Mar. Pollut. Bull.* **62**: 2512– 9.
CrossrefCASPubMedWeb of Science®Google Scholar
Accoroni, S., Romagnoli, T., Pichierri, S., Colombo, F. & Totti, C. 2012b. Morphometric analysis of *Ostreopsis* cf. *ovata* cells in relation to environmental conditions and bloom phases. *Harmful Algae* **19**: 15– 22.
CrossrefWeb of Science®Google Scholar
Accoroni, S., Romagnoli, T., Pichierri, S. & Totti, C. 2014. New insights on the life cycle stages of the toxic benthic dinoflagellate Ostreopsis cf. ovata. *Harmful Algae* **34**: 7– 16.
CrossrefWeb of Science®Google Scholar
Accoroni, S., Romagnoli, T., Pichierri, S. & Totti, C. 2016. Effects of the bloom of harmful benthic dinoflagellate *Ostreopsis* cf. *ovata* on the microphytobenthos community in the northern Adriatic Sea. *Harmful Algae* **55**: 179– 90.
CrossrefPubMedWeb of Science®Google Scholar
Accoroni, S. & Totti, C. 2016. The toxic benthic dinoflagellates of the genus *Ostreopsis* in temperate areas: a review. *Adv. Oceanogr. Limnol.* **7**: 1– 15.
CrossrefCASGoogle Scholar
Aligizaki, K., Katikou, P., Nikolaidis, G. & Panou, A. 2008. First episode of shellfish contamination by palytoxin-like compounds from *Ostreopsis* species (Aegean Sea, Greece). *Toxicon* **51**: 418– 27.
CrossrefCASPubMedWeb of Science®Google Scholar
Aligizaki, K. & Nikolaidis, G. 2006. The presence of the potentially toxic genera *Ostreopsis* and *Coolia* (Dinophyceae) in the north Aegean Sea, Greece. *Harmful Algae* **5**: 717– 30.
CrossrefWeb of Science®Google Scholar
Amorim, A., Veloso, V. & Penna, A. 2010. First detection of *Ostreopsis* cf. *siamensis* in Portuguese coastal waters. *Harmful Algae News* **42**: 6– 7.
Google Scholar
Balech, E. 1980. On thecal morphology of dinoflagellates with special emphasis on circular and sulcal plates. *An. Centro Cienc. Mar. Limnol. Univ. Nat. Autón. México* **7**: 57– 68.
Google Scholar
Battocchi, C., Totti, C., Vila, M., Masó, M., Capellacci, S., Accoroni, S., Reñé, A., Scardi, M. & Penna, A. 2010. Monitoring toxic microalgae *Ostreopsis* (dinoflagellate) species in coastal waters of the Mediterranean Sea using molecular PCR-based assay combined with light microscopy. *Mar. Pollut. Bull.* **60**: 1074– 84.

CrossrefCASPubMedWeb of Science®Google Scholar
Bennouna, A., El Attar, J., Abouabdellah, R., Palma, S., Penna, A. & Moita, T. 2010. First records of *Ostreopsis* cf. *siamensis* in Moroccan Atlantic upwelling waters. *Harmful Algae News* **42**: 1– 3.
Google Scholar
Besada, E. G., Loeblich, L. A. & Loeblich, A. R. 1982. Observations on tropical, benthic dinoflagellates from ciguatera-endemic areas - *Coolia*, *Gambierdiscus* and *Ostreopsis*. *Bull. Mar. Sci.* **32**: 723– 35.
Web of Science®Google Scholar
Bomber, J. W. & Aikman, K. E. 1989. The ciguatera dinoflagellates. *Biological Oceanography* **6**: 291– 311.
Google Scholar
Bravo, I., Vila, M., Casabianca, S., Rodriguez, F., Rial, P., Riobó, P. & Penna, A. 2012. Life cycle stages of the benthic palytoxin-producing dinoflagellate *Ostreopsis* cf. *ovata* (Dinophyceae). *Harmful Algae* **18**: 24– 34.
CrossrefCASWeb of Science®Google Scholar
Brissard, C., Hervé, F., Sibat, M., Séchet, V., Hess, P., Amzil, Z. & Herrenknecht, C. 2015. Characterization of ovatoxin-h, a new ovatoxin analog, and evaluation of chromatographic columns for ovatoxin analysis and purification. *J. Chromatogr. A* **1388**: 87– 101.
CrossrefCASPubMedWeb of Science®Google Scholar
Carella, F., Sardo, A., Mangoni, O., Di Cioccio, D., Urciuolo, G., De Vico, G. & Zingone, A. 2015. Quantitative histopathology of the Mediterranean mussel (*Mytilus galloprovincialis* L.) exposed to the harmful dinoflagellate *Ostreopsis* cf. *ovata*. *J. Invertebr. Pathol.* **127**: 130– 40.
CrossrefCASPubMedWeb of Science®Google Scholar
Carlson, R. D. & Tindall, D. R. 1985. Distribution and periodicity of toxic dinoflagellates in the Virgin Islands. *In* D. M. Anderson, A. W. White & D. G. Baden [Eds.] *Toxic Dinoflagellates*. Elsevier, Amsterdam, the Netherlands, pp. 171– 6.
Google Scholar
Carnicer, O., Guallar, C., Andree, K. B., Diogène, J. & Fernández-Tejedor, M. 2015. *Ostreopsis* cf. *ovata* dynamics in the NW Mediterranean Sea in relation to biotic and abiotic factors. *Environ. Res.* **143**(Part B): 89– 99.
CrossrefCASPubMedWeb of Science®Google Scholar
Casabianca, S., Casabianca, A., Riobó, P., Franco, J. M., Vila, M. & Penna, A. 2013. Quantification of the toxic dinoflagellate *Ostreopsis* spp. by qPCR assay in marine aerosol. *Environ. Sci. Technol.* **47**: 3788– 95.
CrossrefCASPubMedWeb of Science®Google Scholar
Chang, F. H., Shimizu, Y., Hay, B., Stewart, R., Mackay, G. & Tasker, R. 2000. Three recently recorded *Ostreopsis* spp. (Dinophyceae) in New Zealand: temporal and regional distribution in the upper North Island from 1995 to 1997. *New Zeal. J. Mar. Fresh.* **34**: 29– 39.
CrossrefWeb of Science®Google Scholar
Ciminiello, P., Dell'Aversano, C., Dello Iacovo, E., Fattorusso, E., Forino, M., Grauso, L. & Tartaglione, L. 2012a. High resolution LC-MSn fragmentation pattern of palytoxin as template to gain new insights into ovatoxin-A structure. The key role of calcium in MS behavior of palytoxins. *J. Am. Soc. Mass Spectr.* **23**: 952– 63.
CrossrefCASPubMedWeb of Science®Google Scholar
Ciminiello, P., Dell'Aversano, C., Dello Iacovo, E., Fattorusso, E., Forino, M., Grauso, L., Tartaglione, L., Guerrini, F. & Pistocchi, R. 2010. Complex palytoxin-like profile of *Ostreopsis ovata*. Identification of four new ovatoxins by high-resolution liquid chromatography/mass spectrometry. *Rapid Commun. Mass Sp.* **24**: 2735– 44.
Wiley Online LibraryCASPubMedWeb of Science®Google Scholar
Ciminiello, P., Dell'Aversano, C., Dello Iacovo, E., Fattorusso, E., Forino, M., Tartaglione, L., Battocchi, C. & Penna, A. 2012b. Unique toxin profile of a Mediterranean *Ostreopsis* cf. *ovata* strain: HR LC-MSn characterization of ovatoxin-f, a new palytoxin congener. *Chem. Res. Toxicol.* **25**: 1243– 52.
CrossrefCASPubMedWeb of Science®Google Scholar
Ciminiello, P., Dell'Aversano, C., Dello Iacovo, E., Fattorusso, E., Forino, M., Tartaglione, L., Benedettini, G. et al. 2014. First finding of *Ostreopsis* cf. *ovata* toxins in marine aerosols. *Environ. Sci. Technol.* **48**: 3532– 40.
CrossrefCASPubMedWeb of Science®Google Scholar
Ciminiello, P., Dell'Aversano, C., Dello Iacovo, E., Forino, M. & Tartaglione, L. 2015. Liquid chromatography–high-resolution mass spectrometry for palytoxins in mussels. *Anal. Bioanal. Chem.* **407**: 1463– 73.
CrossrefCASPubMedWeb of Science®Google Scholar
Ciminiello, P., Dell'Aversano, C., Fattorusso, E., Forino, M., Magno, G. S., Tartaglione, L., Grillo, C. & Melchiorre, N. 2006. The Genoa 2005 outbreak. Determination of putative palytoxin in

Mediterranean *Ostreopsis ovata* by a new liquid chromatography tandem mass spectrometry method. *Anal. Chem.* **78**: 6153– 9.
CrossrefCASPubMedWeb of Science®Google Scholar
Ciminiello, P., Dell'Aversano, C., Iacovo, E. D., Fattorusso, E., Forino, M., Tartaglione, L., Yasumoto, T., Battocchi, C., Giacobbe, M., Amorim, A. & Penna, A. 2013. Investigation of toxin profile of Mediterranean and Atlantic strains of *Ostreopsis* cf. *siamensis* (Dinophyceae) by liquid chromatography-high resolution mass spectrometry. *Harmful Algae* **23**: 19– 27.
CrossrefCASWeb of Science®Google Scholar
Coats, D. W. 2002. Dinoflagellate life-cycle complexities. *J. Phycol.* **38**: 417– 9.
Wiley Online LibraryWeb of Science®Google Scholar
Cohu, S., Mangialajo, L., Thibaut, T., Blanfuné, A., Marro, S. & Lemée, R. 2013. Proliferation of the toxic dinoflagellate *Ostreopsis* cf. *ovata* in relation to depth, biotic substrate and environmental factors in the North West Mediterranean Sea. *Harmful Algae* **24**: 32– 44.
CrossrefWeb of Science®Google Scholar
Darriba, D., Taboada, G. L., Doallo, R. & Posada, D. 2012. jModelTest 2: more models, new heuristics and parallel computing. *Nat. Methods* **9**: 772.
CrossrefCASPubMedWeb of Science®Google Scholar
David, H., Laza-Martinez, A., Miguel, I. & Orive, E. 2013. *Ostreopsis* cf. *siamensis* and *Ostreopsis* cf. *ovata* from the Atlantic Iberian Peninsula: morphological and phylogenetic characterization. *Harmful Algae* **30**: 44– 55.
CrossrefCASWeb of Science®Google Scholar
Del Favero, G., Sosa, S., Pelin, M., D'Orlando, E., Florio, C., Lorenzon, P., Poli, M. & Tubaro, A. 2012. Sanitary problems related to the presence of *Ostreopsis* spp. in the Mediterranean Sea: a multidisciplinary scientific approach. *Ann Ist Super Sanità* **48**: 407– 14.
CrossrefCASPubMedWeb of Science®Google Scholar
Dell'Aversano, C., Tartaglione, L., Dello Iacovo, E., Forino, M., Casabianca, S., Penna, A. & Ciminiello, P. 2015. *Ostreopsis* cf. *ovata* from the Mediterranean Sea. Variability in toxin profiles and structural elucidation of unknowns through LC-HRMS^n. *In* A. L. MacKenzie [Ed.] *Marine and Freshwater Harmful Algae. Proceedings of the 16th International Conference on Harmful Algae, Wellington, New Zealand 27th-31st October 2014*. Cawthron Institute, Nelson, New Zealand and International Society for the Study of Harmful Algae (ISSHA), ISBN 978-87-990827-5-9; pp. 70– 3.
Google Scholar
Edler, L. & Elbrachter, M. 2010. The Utermöhl method for quantitative phytoplankton analysis. *In* B. Karlson, C. Cusack & E. Bresnan [Eds.] *Microscopic and Molecular Methods for Quantitative Phytoplankton Analysis*. UNESCO, Paris (IOC Manuals and Guides, no. 55), pp. 13– 20.
Google Scholar
Escalera, L., Benvenuto, G., Scalco, E., Zingone, A. & Montresor, M. 2014. Ultrastructural features of the benthic dinoflagellate *Ostreopsis* cf. *ovata* (Dinophyceae). *Protist* **165**: 260– 74.
CrossrefPubMedWeb of Science®Google Scholar
Faimali, M., Giussani, V., Piazza, V., Garaventa, F., Corrà, C., Asnaghi, V., Privitera, D., Gallus, L., Cattaneo-Vietti, R., Mangialajo, L. & Chiantore, M. 2012. Toxic effects of harmful benthic dinoflagellate *Ostreopsis ovata* on invertebrate and vertebrate marine organisms. *Mar. Environ. Res.* **76**: 97– 107.
CrossrefCASPubMedWeb of Science®Google Scholar
Faust, M. A. 1999. Three new *Ostreopsis* species (Dinophyceae): *O. marinus* sp. nov., *O. belizeanus* sp. nov., and *O. carribeanus* sp. nov. *Phycologia* **38**: 92– 9.
CrossrefWeb of Science®Google Scholar
Faust, M. A. & Morton, S. L. 1995. Morphology and ecology of the marine dinoflagellate *Ostreopsis labens* sp. nov. (Dinophyceae). *J. Phycol.* **31**: 456– 63.
Wiley Online LibraryWeb of Science®Google Scholar
Faust, M. A., Morton, S. L. & Quod, J. P. 1996. Further SEM study of marine dinoflagellates: the genus *Ostreopsis* (Dinophyceae). *J. Phycol.* **32**: 1053– 65.
Wiley Online LibraryWeb of Science®Google Scholar
Fensome, R. A., Taylor, F. J. R., Norris, G., Sarjeant, W. A. S., Wharton, D. I. & Williams, G. L. 1993. *A Classification of Living and Fossil Dinoflagellates*. Micropaleontology, Special Publication Number 7. Sheridan Press, Hanover, Pennsylvania, 351 pp.
Google Scholar
Fraga, S. & Rodríguez, F. 2014. Genus *Gambierdiscus* in the Canary Islands (NE Atlantic Ocean) with description of *Gambierdiscus silvae* sp. nov., a new potentially toxic epiphytic benthic dinoflagellate. *Protist* **165**: 839– 53.

CrossrefPubMedWeb of Science®Google Scholar
Fraga, S., Rodriguez, F., Caillaud, A., Diogene, J., Raho, N. & Zapata, M. 2011. *Gambierdiscus excentricus* sp. nov. (Dinophyceae), a benthic toxic dinoflagellate from the Canary Islands (NE Atlantic Ocean). *Harmful Algae* **11**: 10– 22.
CrossrefWeb of Science®Google Scholar
Fukuyo, Y. 1981. Taxonomical study on benthic dinoflagellates collected in coral reefs. *Bull. Jap. Soc. Sci. Fish.* **47**: 967– 78.
CrossrefWeb of Science®Google Scholar
Gallitelli, M., Ungaro, N., Addante, L. M., Silver, N. G. & Sabba, C. 2005. Respiratory illness as a reaction to tropical algal blooms occurring in a temperate climate. *J. Am. Med. Assoc.* **293**: 2599– 600.
CrossrefCASPubMedWeb of Science®Google Scholar
García-Altares, M., Tartaglione, L., Dell'Aversano, C., Carnicer, O., De La Iglesia, P., Forino, M., Diogène, J. & Ciminiello, P. 2015. The novel ovatoxin-g and isobaric palytoxin (so far referred to as putative palytoxin) from *Ostreopsis* cf. *ovata* (NW Mediterranean Sea): structural insights by LC-high resolution MS^n. *Anal. Bioanal. Chem.* **407**: 1191– 204.
CrossrefCASPubMedWeb of Science®Google Scholar
Giussani, V., Sbrana, F., Asnaghi, V., Vassalli, M., Faimali, M., Casabianca, S., Penna, A. et al. 2015. Active role of the mucilage in the toxicity mechanism of the harmful benthic dinoflagellate *Ostreopsis* cf. *ovata*. *Harmful Algae* **44**: 46– 53.
CrossrefCASWeb of Science®Google Scholar
Glibert, P. M., Allen, J. I., Bouwman, A. F., Brown, C. W., Flynn, K. J., Lewitus, A. J. & Madden, C. J. 2010. Modeling of HABs and eutrophication Status, advances, challenges. *J. Marine Syst.* **83**: 262– 75.
CrossrefWeb of Science®Google Scholar
Glibert, P. M. & Burkholder, J. M. 2006. The complex relationships between increases in fertilization of the earth, coastal eutrophication and proliferation of Harmful Algal Blooms. *In* E. Granéli & J. T. Turner [Eds.] *Ecology of Harmful Algae*. Springer Berlin Heidelberg, Heidelberg, Germany, pp. 341– 54.
CrossrefGoogle Scholar
Gorbi, S., Avio, G. C., Benedetti, M., Totti, C., Accoroni, S., Pichierri, S., Bacchiocchi, S., Orletti, R., Graziosi, T. & Regoli, F. 2013. Effects of harmful dinoflagellate *Ostreopsis* cf. *ovata* exposure on immunological, histological and oxidative responses of mussels *Mytilus galloprovincialis*. *Fish Shellfish Immun.* **35**: 941– 50.
CrossrefCASWeb of Science®Google Scholar
Gorbi, S., Bocchetti, R., Binelli, A., Bacchiocchi, S., Orletti, R., Nanetti, L., Raffaelli, F., Vignini, A., Accoroni, S., Totti, C. & Regoli, F. 2012. Biological effects of palytoxin-like compounds from *Ostreopsis* cf. *ovata*: a multibiomarkers approach with mussels *Mytilus galloprovincialis*. *Chemosphere* **89**: 623– 32.
CrossrefCASPubMedWeb of Science®Google Scholar
Guerrini, F., Pezzolesi, L., Feller, A., Riccardi, M., Ciminiello, P., Dell'Aversano, C., Tartaglione, L., Dello Iacovo, E., Fattorusso, E., Forino, M. & Pistocchi, R. 2010. Comparative growth and toxin profile of cultured *Ostreopsis ovata* from the Tyrrhenian and Adriatic Seas. *Toxicon* **55**: 211– 20.
CrossrefCASPubMedWeb of Science®Google Scholar
Guillard, R. R. L. 1975. Culture of phytoplankton for feeding marine invertebrates. *In* W. L. Smith & M. H. Chanley [Eds.] *Culture of Marine Invertebrates Animals*. Plenum Press, New York, pp. 26– 60.
CrossrefGoogle Scholar
Guillard, R. R. L. 1978. Counting slides. *In* A. Sournia [Ed.] *Phytoplankton Manual. Monographs on Oceanographic Methodology 6*. UNESCO, Paris, pp. 182– 9.
Google Scholar
Guindon, S., Dufayard, J. F., Lefort, V., Anisimova, M., Hordijk, W. & Gascuel, O. 2010. New algorithms and methods to estimate maximum-likelihood phylogenies, assessing the performance of PhyML 3.0. *Syst. Biol.* **59**: 307– 21.
CrossrefCASPubMedWeb of Science®Google Scholar
Heisler, J., Glibert, P. M., Burkholder, J. M., Anderson, D. M., Cochlan, W., Dennison, W. C., Dortch, Q. et al. 2008. Eutrophication and harmful algal blooms: a scientific consensus. *Harmful Algae* **8**: 3– 13.
CrossrefCASPubMedWeb of Science®Google Scholar
Holmes, M. J., Gillespie, N. C. & Lewis, R. J. 1988. Toxicity and morphology of *Ostreopsis* cf. *siamensis* cultured from a ciguatera endemic region of Queensland, Australia. *In* J. H. Choat, D. Barnes, M. A. Borowitzka, J. C. Coll, P. J. Davies, P. Flood, B. G. Hatcher, D. Hopley, P. A. Hutchings, D. Kinsey, G. R. Orme, M. Pichon, P. F. Sale, P. Sammarco, C. C. Wallace, C. Wilkinson, E. Wolanski & O. Bellwood [Eds.] *Proceedings of the 6th International Coral Reef Symposium*. vol. 3. Australian Institute of Marine Science, Townsville, Australia, pp. 49– 54.

Google Scholar
Hoppenrath, M., Murray, S. A., Chomérat, N. & Horiguchi, T. 2014. *Marine Benthic Dinoflagellates - Unveiling their Worldwide Biodiversity*. Kleine Senckenberg-Reihe, Band 54, Schweizerbart, Stuttgart, Germany, 276 pp.
Google Scholar
Hoshaw, R. W. & Rosowski, J. R. 1973. Methods for microscopic algae. *In* J. R. Stein [Ed.] *Handbook of Phycological Methods*. Cambridge University Press, New York, pp. 53– 67.
Google Scholar
Illoul, H., Hernandez, F. R., Vila, M., Adjas, N., Younes, A. A., Bournissa, M., Koroghli, A., Marouf, N., Rabia, S. & Ameur, F. L. K. 2012. The genus *Ostreopsis* along the Algerian coastal waters (SW Mediterranean Sea) associated with a human respiratory intoxication episode. *Cryptogam. Algologie* **33**: 209– 16.
CrossrefWeb of Science®Google Scholar
Ismael, A. & Halim, Y. 2012. Potentially harmful *Ostreopsis* spp. In the coastal waters of Alexandria-Egypt. *Mediterr. Mar. Sci.* **13**: 208– 12.
CrossrefWeb of Science®Google Scholar
Kang, N. S., Jeong, H. J., Lee, S. Y., Lim, A. S., Lee, M. J., Kim, H. S. & Yih, W. 2013. Morphology and molecular characterization of the epiphytic benthic dinoflagellate *Ostreopsis* cf. *ovata* in the temperate waters off Jeju Island, Korea. *Harmful Algae* **27**: 98– 112.
CrossrefCASWeb of Science®Google Scholar
Kermarec, F., Dor, F., Armengaud, A., Charlet, F., Kantin, R., Sauzade, D. & De Haro, L. 2008. Les risques sanitaires liés à la présence d'*Ostreopsis ovata* dans les eaux de baignade ou d'activités nautiques. *Environnement, Risques & Santé* **7**: 357– 63.
Web of Science®Google Scholar
Laza-Martinez, A., Orive, E. & Miguel, I. 2011. Morphological and genetic characterization of benthic dinoflagellates of the genera *Coolia*, *Ostreopsis* and *Prorocentrum* from the south-eastern Bay of Biscay. *Eur. J. Phycol.* **46**: 45– 65.
CrossrefWeb of Science®Google Scholar
Lenoir, S., Ten-Hage, L., Turquet, J., Quod, J. P., Bernard, C. & Hennion, M. C. 2004. First evidence of palytoxin analogues from an *Ostreopsis mascarenensis* (Dinophyceae) benthic bloom in Southwestern Indian Ocean. *J. Phycol.* **40**: 1042– 51.
Wiley Online LibraryCASWeb of Science®Google Scholar
Litaker, R. W., Vandersea, M. W., Faust, M. A., Kibler, S. R., Chinain, M., Holmes, M. J., Holland, W. C. & Tester, P. A. 2009. Taxonomy of *Gambierdiscus* including four new species, *Gambierdiscus caribaeus*, *Gambierdiscus carolinianus*, *Gambierdiscus carpenteri* and *Gambierdiscus ruetzleri* (Gonyaulacales, Dinophyceae). *Phycologia* **48**: 344– 90.
CrossrefWeb of Science®Google Scholar
Mabrouk, L., Hamza, A., Brahim, M. B. & Bradai, M. N. 2011. Temporal and depth distribution of microepiphytes on *Posidonia oceanica* (L.) Delile leaves in a meadow off Tunisia. *Mar. Ecol. Evol. Persp.* **32**: 148– 61.
Wiley Online LibraryWeb of Science®Google Scholar
Mabrouk, L., Hamza, A., Mahfoudi, M. & Bradai, M. N. 2012. Spatial and temporal variations of epiphytic *Ostreopsis siamensis* on *Posidonia oceanica* (L.) Delile leaves in Mahdia (Tunisia). *Cah. Biol. Mar.* **53**: 419– 27.
Web of Science®Google Scholar
Mangialajo, L., Bertolotto, R., Cattaneo-Vietti, R., Chiantore, M., Grillo, C., Lemée, R., Melchiorre, N., Moretto, P., Povero, P. & Ruggieri, N. 2008. The toxic benthic dinoflagellate *Ostreopsis ovata*: quantification of proliferation along the coastline of Genoa, Italy. *Mar. Pollut. Bull.* **56**: 1209– 14.
CrossrefCASPubMedWeb of Science®Google Scholar
Mangialajo, L., Ganzin, N., Accoroni, S., Asnaghi, V., Blanfuné, A., Cabrini, M., Cattaneo-Vietti, R. et al. 2011. Trends in *Ostreopsis* proliferation along the Northern Mediterranean coasts. *Toxicon* **57**: 408– 20.
CrossrefCASPubMedWeb of Science®Google Scholar
Mercado, J. A., Rivera-Rentas, A. L., Gonzalez, I., Tosteson, T. R., Molgo, J. & Escalona de Motta, G. 1994. Neuro-and myo-toxicity of extracts from the benthic dinoflagellate *Ostreopsis lenticularis* is sensitive to μ-conotoxin. *Soc. Neurosci. Abstr.* **20**: 718.
Google Scholar

Meunier, F. A., Mercado, J. A., Molgó, J., Tosteson, T. R. & Escalona de Motta, G. 1997. Selective depolarization of the muscle membrane in frog nerve-muscle preparations by a chromatographically purified extract of the dinoflagellate *Ostreopsis lenticularis*. *Brit. J. Pharmacol.* **121**: 1224– 30.
Wiley Online LibraryCASPubMedWeb of Science®Google Scholar
Mohammad-Noor, N., Moestrup, Ø., Lundholm, N., Fraga, S., Adam, A., Holmes, M. J. & Saleh, E. 2013. Autecology and phylogeny of *Coolia tropicalis* and *Coolia malayensis* (Dinophyceae), with emphasis on taxonomy of *C. tropicalis* based on light microscopy, scanning electron microscopy and LSU rDNA. *J. Phycol.* **49**: 536– 45.
Wiley Online LibraryPubMedWeb of Science®Google Scholar
Monti, M., Minocci, M., Beran, A. & Ivesa, L. 2007. First record of *Ostreopsis* cfr. *ovata* on macroalgae in the Northern Adriatic Sea. *Mar. Pollut. Bull.* **54**: 598– 601.
CrossrefCASPubMedWeb of Science®Google Scholar
Murphy, J. & Riley, J. P. 1962. A modified single solution method for the determination of phosphate in natural waters. *Anal. Chim. Acta* **27**: 31– 6.
CrossrefCASPubMedGoogle Scholar
Nakajima, I., Oshima, Y. & Yasumoto, T. 1981. Toxicity of benthic dinoflagellates in Okinawa. *Nippon Suisan Gakk.* **47**: 1029– 33.
CrossrefWeb of Science®Google Scholar
Nascimento, S. M., Corrêa, E. V., Menezes, M., Varela, D., Paredes, J. & Morris, S. 2012. Growth and toxin profile of *Ostreopsis* cf. *ovata* (Dinophyta) from Rio de Janeiro, Brazil. *Harmful Algae* **13**: 1– 9.
CrossrefCASWeb of Science®Google Scholar
Norris, D. R., Bomber, J. W. & Balech, E. 1985. Benthic dinoflagellates associated with ciguatera from Florida Keys. I. *Ostreopsis heptagona* sp. nov. *In* D. M. Anderson, A. W. White & D. G. Baden [Eds.] *Toxic Dinoflagellates*. Elsevier, Amsterdam, the Netherlands, pp. 39– 44.
Google Scholar
Pagliara, P. & Caroppo, C. 2012. Toxicity assessment of *Amphidinium carterae*, *Coolia* cfr. *monotis* and *Ostreopsis* cfr. *ovata* (Dinophyta) isolated from the northern Ionian Sea (Mediterranean Sea). *Toxicon* **60**: 1203– 14.
CrossrefCASPubMedWeb of Science®Google Scholar
Parsons, M. L., Aligizaki, K., Bottein, M. Y. D., Fraga, S., Morton, S. L., Penna, A. & Rhodes, L. 2012. *Gambierdiscus* and *Ostreopsis*: reassessment of the state of knowledge of their taxonomy, geography, ecophysiology, and toxicology. *Harmful Algae* **14**: 107– 29.
CrossrefCASWeb of Science®Google Scholar
Pearce, I., Marshall, J. A. & Hallegraeff, G. 2001. Toxic epiphytic dinoflagellates from east coast Tasmania, Australia. *In* G. Hallegraeff, S. I. Blackburn, C. J. Bolch & R. J. Lewis [Eds.] *Harmful Algal Blooms 2000*. Intergovernmental Oceanographic Commission of UNESCO, Paris, France, pp. 54– 7.
Google Scholar
Pelin, M., Forino, M., Brovedani, V., Tartaglione, L., Dell'Aversano, C., Pistocchi, R., Poli, M., Sosa, S., Florio, C., Ciminiello, P. & Tubaro, A. 2016. Ovatoxin-a, a palytoxin analogue isolated from *Ostreopsis* cf. *ovata* Fukuyo: cytotoxic activity and ELISA detection. *Environ. Sci. Technol.* **50**: 1544– 51.
CrossrefCASPubMedWeb of Science®Google Scholar
Penna, A., Battocchi, C., Capellacci, S., Fraga, S., Aligizaki, K., Lemée, R. & Vernesi, C. 2014. Mitochondrial, but not rDNA, genes fail to discriminate dinoflagellate species in the genus *Ostreopsis*. *Harmful Algae* **40**: 40– 50.
CrossrefCASWeb of Science®Google Scholar
Penna, A., Fraga, S., Battocchi, C., Casabianca, S., Giacobbe, M. G., Riobó, P. & Vernesi, C. 2010. A phylogeographical study of the toxic benthic dinoflagellate genus *Ostreopsis* Schmidt. *J. Biogeogr.* **37**: 830– 41.
Wiley Online LibraryWeb of Science®Google Scholar
Penna, A., Fraga, S., Battocchi, C., Casabianca, S., Perini, F., Samuela, C., Casabianca, A. et al. 2012. Genetic diversity of the genus *Ostreopsis* Schmidt: phylogeographical considerations and molecular methodology applications for field detection in the Mediterranean Sea. *Cryptogamie Algol.* **33**: 153– 63.
CrossrefWeb of Science®Google Scholar
Penna, A., Vila, M., Fraga, S., Giacobbe, M. G., Andreoni, F., Riobó, P. & Vernesi, C. 2005. Characterization of *Ostreopsis* and *Coolia* (Dinophyceae) isolates in the western Mediterranean Sea based on morphology, toxicity and internal transcribed spacer 5.8s rDNA sequences. *J. Phycol.* **41**: 212– 25.
Wiley Online LibraryCASWeb of Science®Google Scholar

Percopo, I., Siano, R., Rossi, R., Soprano, V., Sarno, D. & Zingone, A. 2013. A new potentially toxic *Azadinium* species (Dinophyceae) from the Mediterranean Sea, *A. dexteroporum* sp. nov.. *J. Phycol.* **49**: 950– 66.
Wiley Online LibraryCASPubMedWeb of Science®Google Scholar
Perini, F., Casabianca, A., Battocchi, C., Accoroni, S., Totti, C. & Penna, A. 2011. New approach using the real-time PCR method for estimation of the toxic marine dinoflagellate *Ostreopsis* cf. *ovata* in marine environment. *PLoS ONE* **6**: e17699.
CrossrefCASPubMedWeb of Science®Google Scholar
Pfannkuchen, M., Godrijan, J., Maric Pfannkuchen, D., Ivesa, L., Kruzic, P., Ciminiello, P., Dell'Aversano, C. et al. 2012. Toxin-producing *Ostreopsis* cf. *ovata* are likely to bloom undetected along coastal areas. *Environ. Sci. Technol.* **46**: 5574– 82.
CrossrefCASPubMedWeb of Science®Google Scholar
Quod, J. P. 1994. *Ostreopsis mascarenensis* sp. nov. (Dinophyceae), dinoflagellé toxique associé a la ciguatera dans l'Océan Indien. *Cryptogamie Algol.* **15**: 243– 51.
Web of Science®Google Scholar
Rhodes, L., Adamson, J., Suzuki, T., Briggs, L. & Garthwaite, I. 2000. Toxic marine epiphytic dinoflagellates, *Ostreopsis siamensis* and *Coolia monotis* (Dinophyceae), in New Zealand. *New Zeal. J. Mar. Fresh.* **34**: 371– 83.
CrossrefWeb of Science®Google Scholar
Ronquist, F. & Huelsenbeck, J. P. 2003. Mrbayes 3: Bayesian phylogenetic inference under mixed models. *Bioinformatics* **19**: 1572– 4.
Wiley Online LibraryCASPubMedWeb of Science®Google Scholar
Sato, S., Nishimura, T., Uehara, K., Sakanari, H., Tawong, W., Hariganeya, N., Smith, K. et al. 2011. Phylogeography of *Ostreopsis* along west Pacific coast, with special reference to a novel clade from Japan. *PLoS ONE* **6**: e27983.
CrossrefCASPubMedWeb of Science®Google Scholar
Scalco, E., Brunet, C., Marino, F., Rossi, R., Soprano, V., Zingone, A. & Montresor, M. 2012. Growth and toxicity responses of Mediterranean *Ostreopsis* cf. *ovata* to seasonal irradiance and temperature conditions. *Harmful Algae* **17**: 25– 34.
CrossrefWeb of Science®Google Scholar
Schmidt, J. 1901. Flora of Koh Chang. Contributions to the knowledge of the vegetation in the Gulf of Siam. *Peridiniales. Bot. Tidsskr.* **24**: 212– 21.
Google Scholar
Selina, M. S., Morozova, T. V., Vyshkvartsev, D. I. & Orlova, T. Y. 2014. Seasonal dynamics and spatial distribution of epiphytic dinoflagellates in Peter the Great Bay (Sea of Japan) with special emphasis on *Ostreopsis* species. *Harmful Algae* **32**: 1– 10.
CrossrefWeb of Science®Google Scholar
Selina, M. S. & Orlova, T. Y. 2010. First occurrence of the genus *Ostreopsis* (Dinophyceae) in the Sea of Japan. *Bot. Mar.* **53**: 243– 9.
CrossrefWeb of Science®Google Scholar
Shears, N. T. & Ross, P. M. 2009. Blooms of benthic dinoflagellates of the genus *Ostreopsis*; an increasing and ecologically important phenomenon on temperate reefs in New Zealand and worldwide. *Harmful Algae* **8**: 916– 25.
CrossrefWeb of Science®Google Scholar
Strickland, J. D. H. & Parsons, T. R. 1968. A practical handbook of seawater analysis. *J. Fish. Res. Board Can.* **167**: 1– 310.
Google Scholar
Tamura, K., Stecher, G., Peterson, D., Filipski, A. & Kumar, S. 2013. MEGA6: Molecular Evolutionary Genetics Analysis version 6.0. *Mol. Biol. Evol.* **30**: 2725– 9.
CrossrefCASPubMedWeb of Science®Google Scholar
Taniyama, S., Arakawa, O., Terada, M., Nishio, S., Takatani, T., Mahmud, Y. & Noguchi, T. 2003. *Ostreopsis* sp., a possible origin of palytoxin (PTX) in parrotfish *Scarus ovifrons*. *Toxicon* **42**: 29– 33.
CrossrefCASPubMedWeb of Science®Google Scholar
Tartaglione, L., Mazzeo, A., Dell'Aversano, C., Forino, M., Giussani, V., Capellacci, S., Penna, A. et al. 2016. Chemical, molecular, and eco-toxicological investigation of *Ostreopsis* sp. from Cyprus Island: structural insights into four new ovatoxins by LC-HRMS/MS. *Anal. Bioanal. Chem.* **408**: 915– 32.
CrossrefCASPubMedWeb of Science®Google Scholar

Tawong, W., Nishimura, T., Sakanari, H., Sato, S., Yamaguchi, H. & Adachi, M. 2014. Distribution and molecular phylogeny of the dinoflagellate genus *Ostreopsis* in Thailand. *Harmful Algae* **37**: 160– 71.
CrossrefWeb of Science®Google Scholar
Throndsen, J. 1978. Preservation and storage. *In* A. Sournia [Ed.] *Phytoplankton Manual. Monographs on Oceanographic Methodology 6*. UNESCO, Paris, pp. 69– 74.
Google Scholar
Tichadou, L., Glaizal, M., Armengaud, A., Grossel, H., Lemee, R., Kantin, R., Lasalle, J. L., Drouet, G., Rambaud, L., Malfait, P. & de Haro, L. 2010. Health impact of unicellular algae of the *Ostreopsis* genus blooms in the Mediterranean Sea: experience of the French Mediterranean coast surveillance network from 2006 to 2009. *Clin. Toxicol.* **48**: 839– 44.
CrossrefPubMedWeb of Science®Google Scholar
Tillmann, U., Elbraechter, M., Krock, B., John, U. & Cembella, A. 2009. *Azadinium spinosum* gen. et sp. nov. (Dinophyceae) identified as a primary producer of azaspiracid toxins. *Eur. J. Phycol.* **44**: 63– 79.
CrossrefCASWeb of Science®Google Scholar
Tosteson, T. R. 1995. The diversity and origins of toxins in ciguatera fish poisoning. *P. R. Health Sci. J.* **14**: 117– 29.
CASPubMedGoogle Scholar
Totti, C., Accoroni, S., Cerino, F., Cucchiari, E. & Romagnoli, T. 2010. *Ostreopsis ovata* bloom along the Conero Riviera (northern Adriatic Sea): relationships with environmental conditions and substrata. *Harmful Algae* **9**: 233– 9.
CrossrefWeb of Science®Google Scholar
Turki, S. 2005. Distribution of toxic dinoflagellates along the leaves of seagrass *Posidonia oceanica* and *Cymodocea nodosa* from the Gulf of Tunis. *Cah. Biol. Mar.* **46**: 29– 34.
Web of Science®Google Scholar
Turki, S., Harzallah, A. & Sammari, C. 2006. Occurrence of harmful dinoflagellates in two different Tunisian ecosystems: the lake of Bizerte and the Gulf of Gabes. *Cah. Biol. Mar.* **47**: 253– 9.
Web of Science®Google Scholar
Uchida, H., Taira, Y. & Yasumoto, T. 2013. Structural elucidation of palytoxin analogs produced by the dinoflagellate *Ostreopsis ovata* IK2 strain by complementary use of positive and negative ion liquid chromatography/quadrupole time-of-flight mass spectrometry. *Rapid Commun. Mass Sp.* **27**: 1999– 2008.
Wiley Online LibraryCASPubMedWeb of Science®Google Scholar
Vila, M., Garcés, E. & Masó, M. 2001. Potentially toxic epiphytic dinoflagellate assemblages on macroalgae in the NW Mediterranean. *Aquat. Microb. Ecol.* **26**: 51– 60.
CrossrefWeb of Science®Google Scholar
Yasumoto, T., Seino, N., Murakami, Y. & Murata, M. 1987. Toxins produced by benthic dinoflagellates. *Biol. Bull.* **172**: 128– 31.
CrossrefCASWeb of Science®Google Scholar

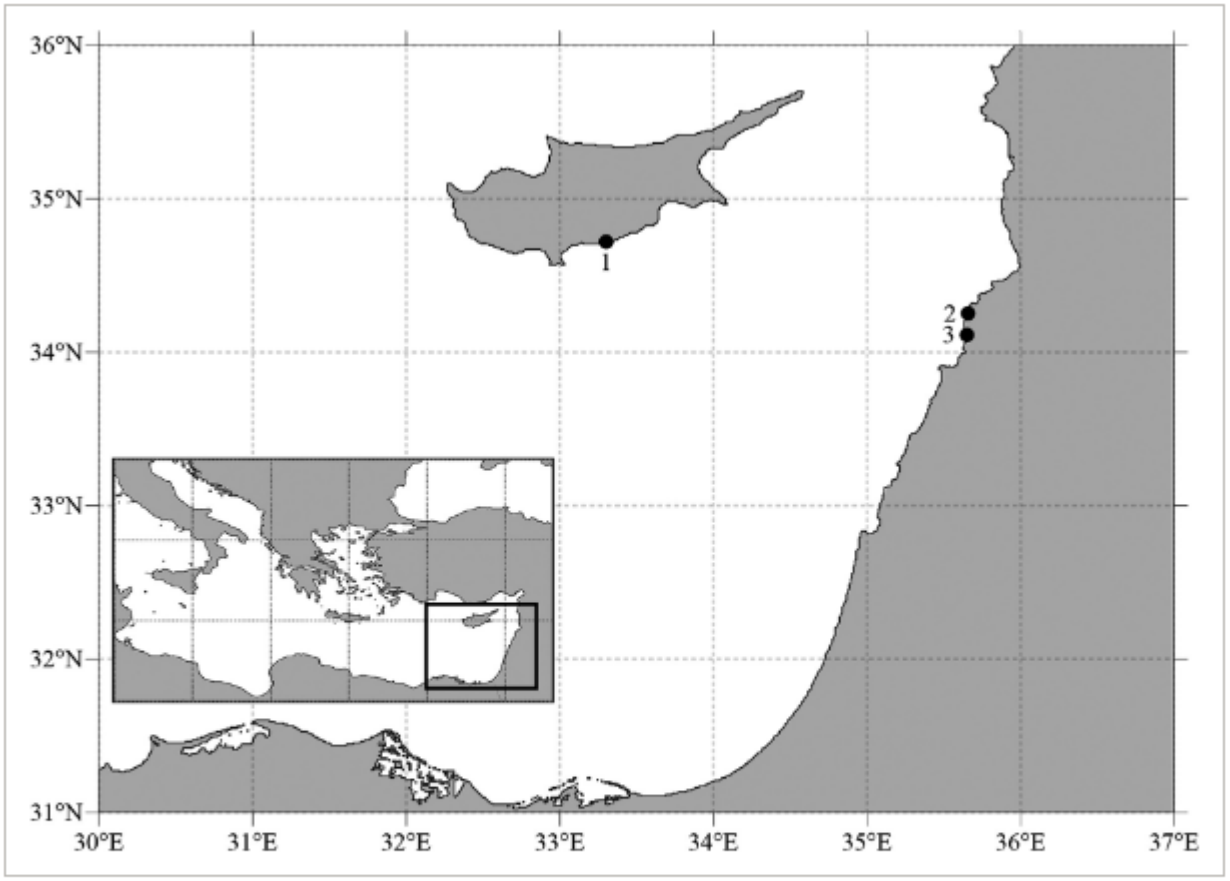

Figure 1

Open in figure viewer | PowerPoint

Map of study area, showing the sites where *Ostreopsis fattorussoi* was found. Site 1: Vassiliko Bay (Cyprus). Site 2: Batroun (Lebanon). Site 3: Byblos (Lebanon).

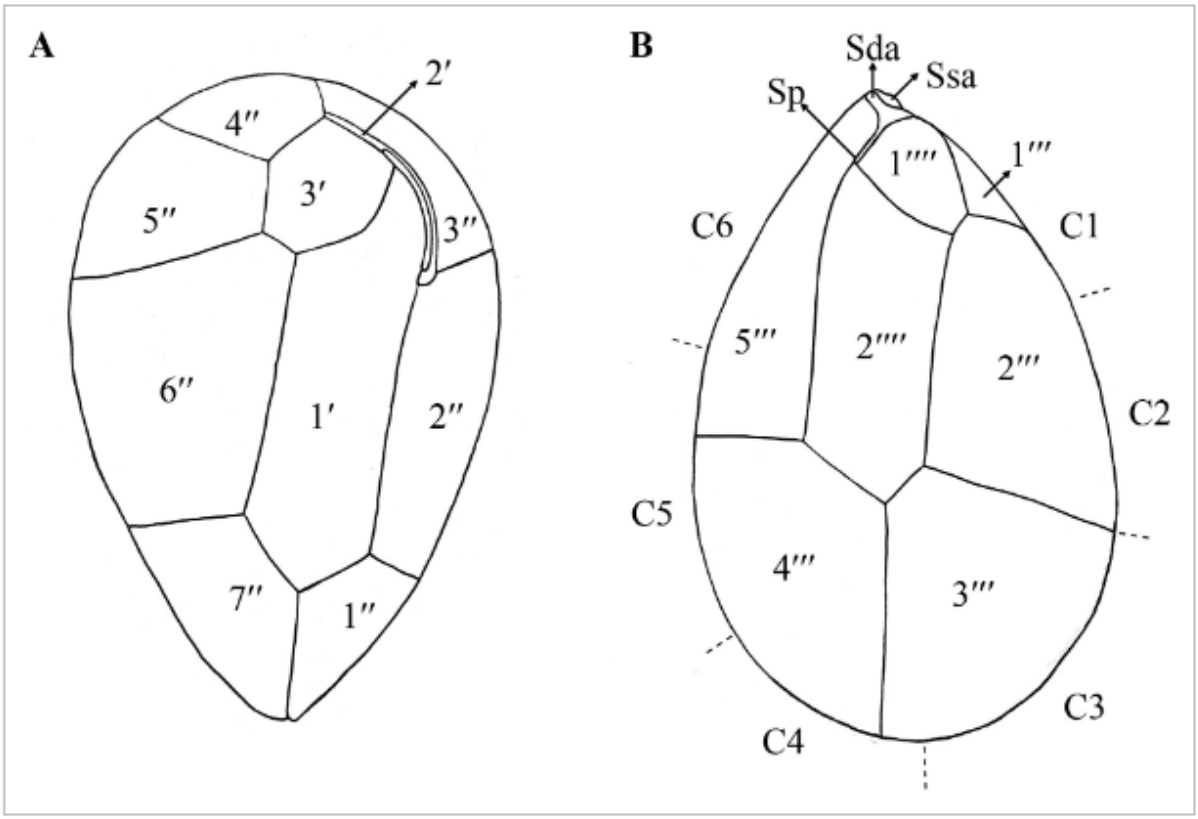

Figure 2

Open in figure viewer | PowerPoint

Ostreopsis fattorussoi. Schematic drawings with plate tabulation of (A) epitheca, (B) hypotheca and cingulum. Sda, right-anterior sulcal; Ssa, left anterior sulcal plate; Sp, posterior sulcal plate.

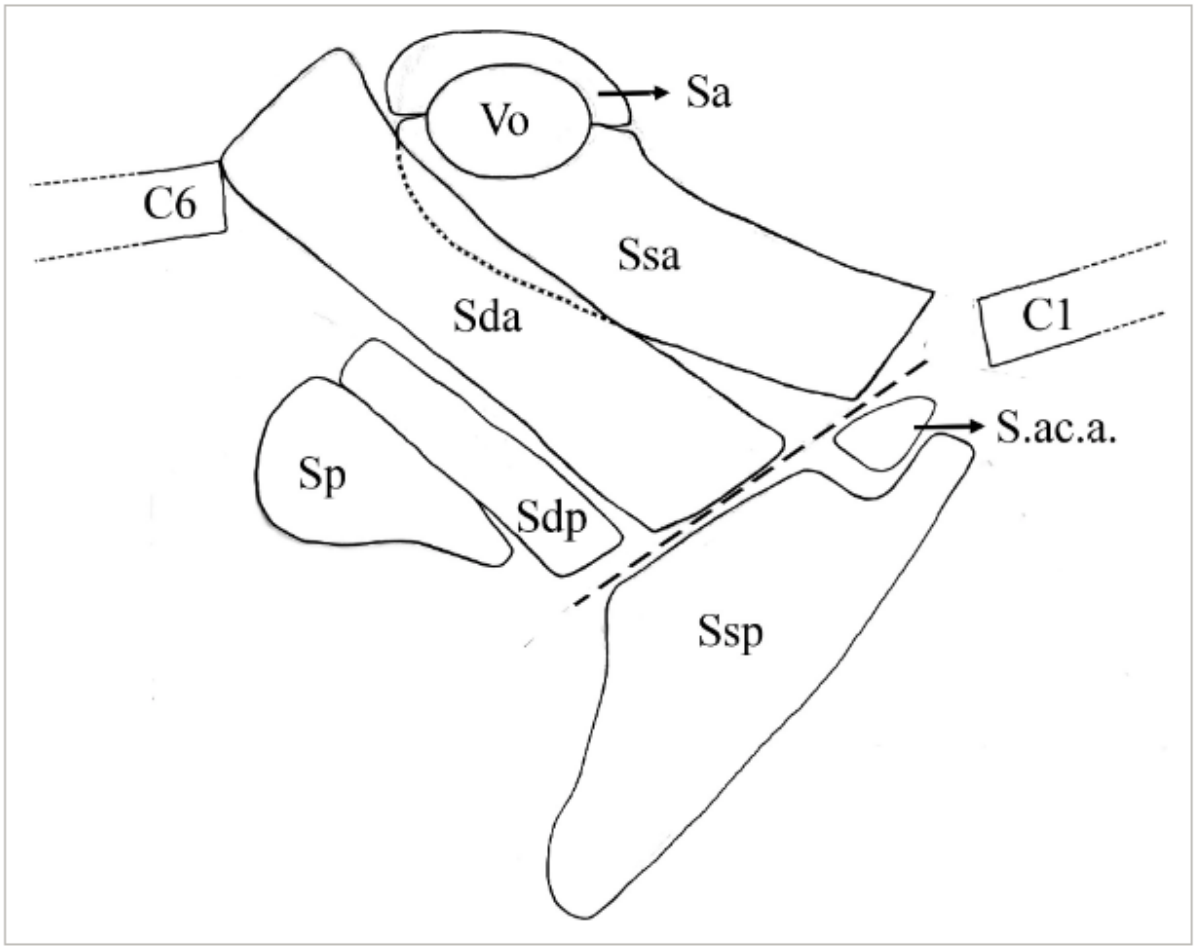

Figure 3

Interpretation drawing of the sulcus of *Ostreopsis fattorussoi*. Sa, anterior sulcal plate; Ssa, left anterior sulcal plate; Sda right-anterior sulcal plate; Sdp, right-posterior sulcal plate; Sp, posterior sulcal plate; Ssp, left posterior sulcal plate; S.ac.a., accessory anterior sulcal plate; dotted line indicates the position of the bottom of the sulcus (Sa, Ssa, Sda, Sdp, and Sp are in the upper side of the sulcus groove and Ssp and S.ac.a. are in the inferior side of the sulcus); Vo, ventral opening.

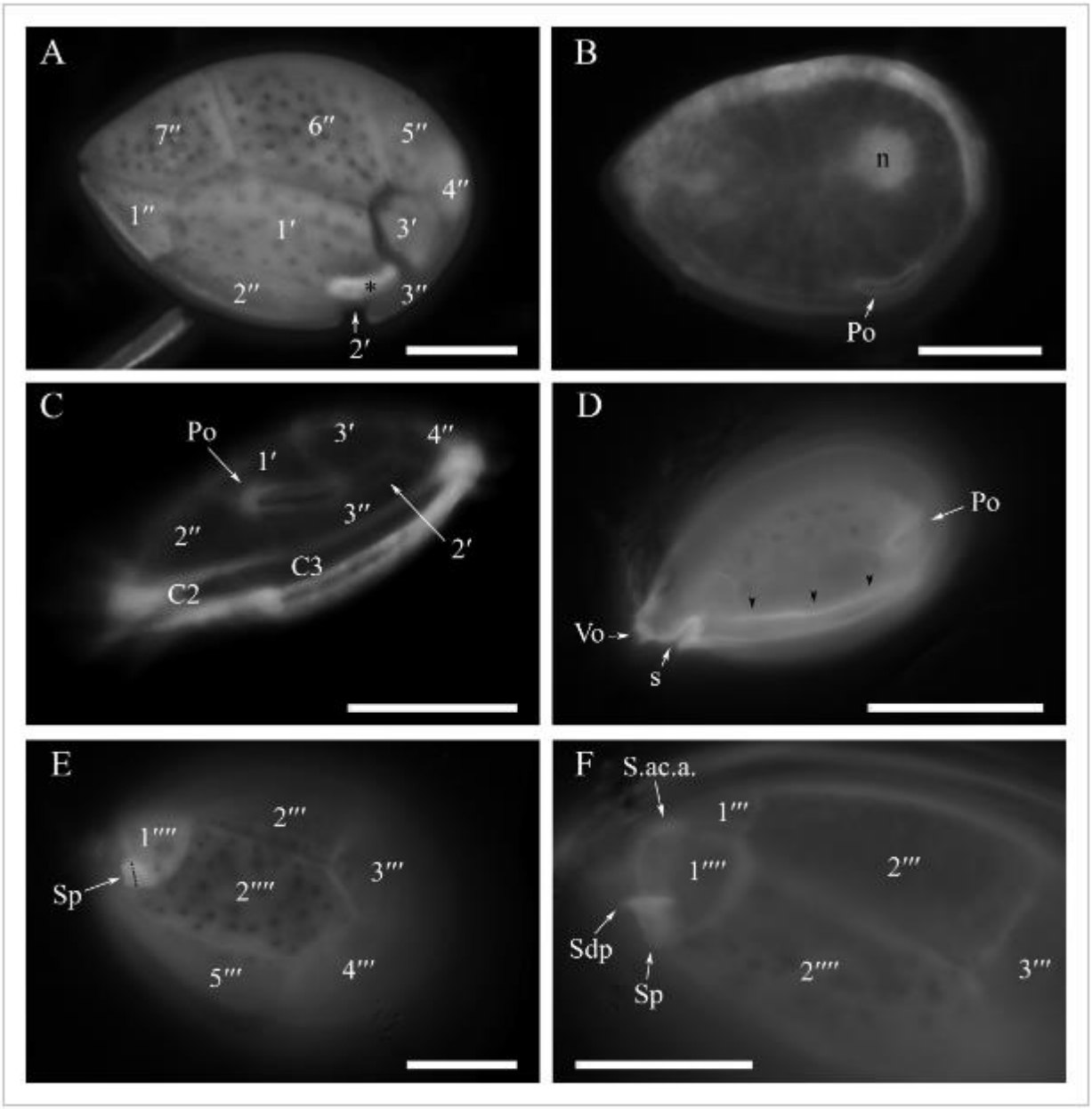

Figure 4

Open in figure viewer | PowerPoint

Ostreopsis fattorussoi, light microscopy micrographs. Epifluorescence observations after Calcofluor-White of cells from natural samples. (A) Epitheca (* = apical pore plate Po). (B) Apical view of a cell stained with SYBR Green highlighting the nucleus (apical pore plate Po is visible). (C) Left lateral view showing the contact of plate 2′ with 4″. (D) Merging of several photograms taken at different foci of the left lateral side of a cell showing the depth of the sulcus (s) and the ventral opening (Vo); arrowheads indicate the cingulum border in the epitheca. (E, F) Hypotheca; (E) focus on the posterior sulcal plate (Sp): although the Sp is almost entirely

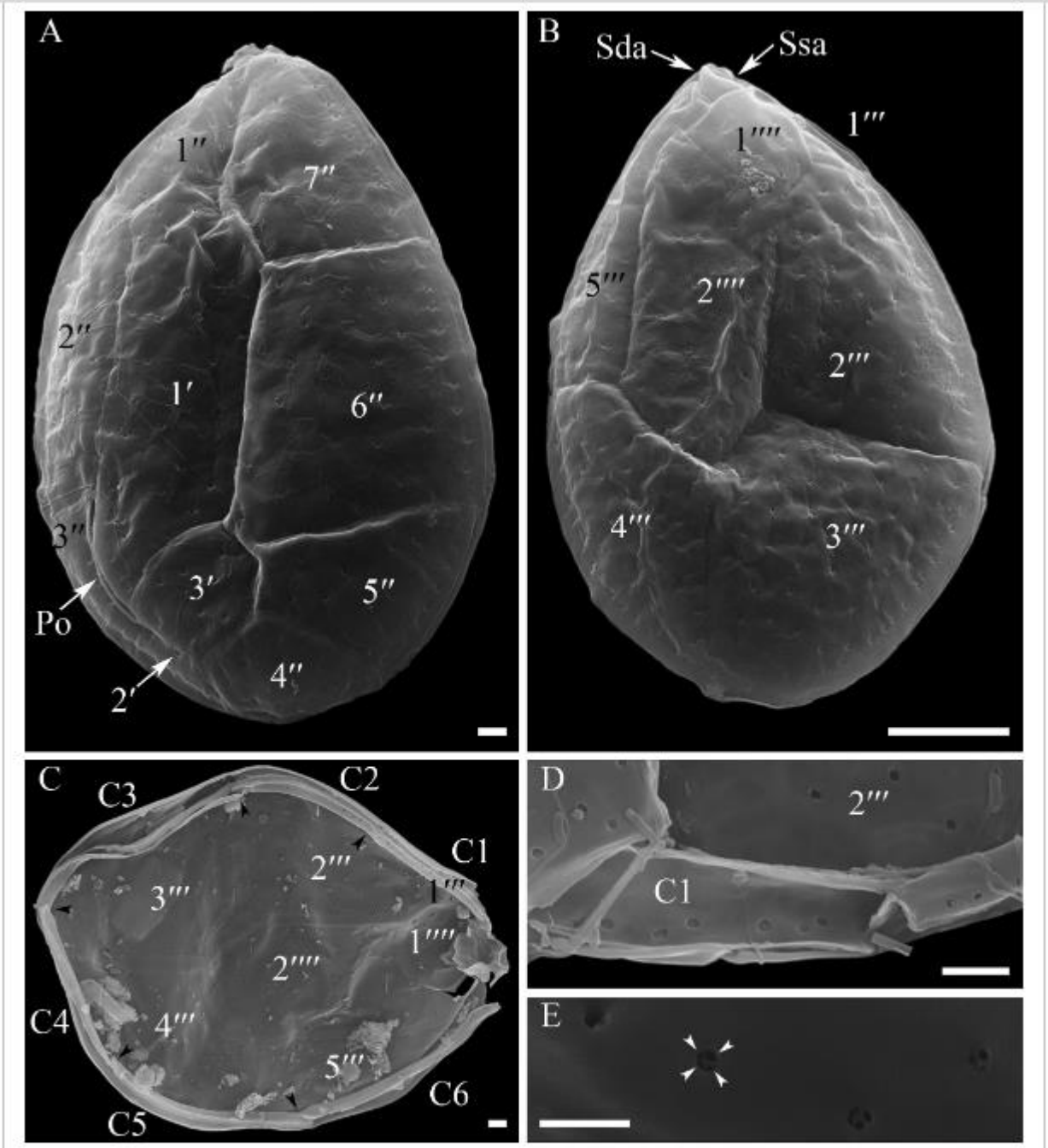

Figure 5

Open in figure viewer | PowerPoint

Ostreopsis fattorussoi, SEM micrographs. (A) Epitheca. (B) Hypotheca. (C) Internal view of the hypotheca showing the cingular plates with distinctive borders (arrowheads) between two adjacent plates. (D, E) Magnification on the internal side of the hypotheca showing the thecal pores; (D) pores lined up along both the borders of the two cingular lists; (E) small perforations inside thecal pores. Po, apical pore plate; Sda, right-anterior sulcal; Ssa, left anterior sulcal plate. Scale bars = 2 μm (A, C, D, and E); 10 μm (B).

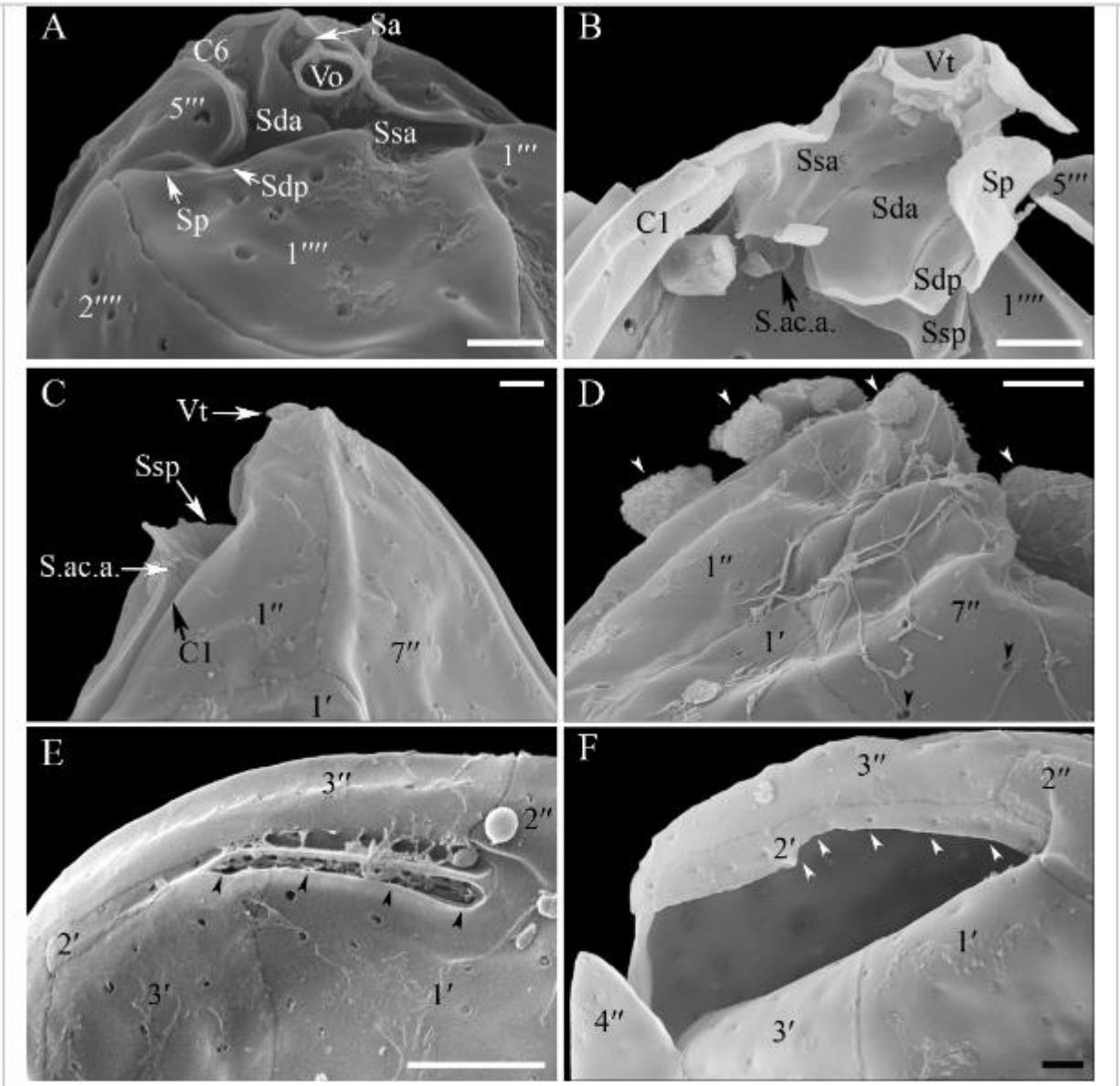

Figure 6

Open in figure viewer | PowerPoint

Ostreopsis fottorussoi, SEM micrographs. (A) Ventral area in an intact cell. (B) Internal view of the hypotheca and the sulcus in a broken cell showing all the sulcal plates (with the exception of Sa): Ssa, Sda, Sdp, and Sp are in the upper side of the sulcus groove and partially cover Ssp and S.ac.a. which are in the inferior side of the sulcus; Sp is unnaturally bended leading show the space between the 1⁗ and 5‴ plates. (C) Left lateral view of the ventral area partially showing the inferior side of the sulcus. (D) Apical ventral view of a cell showing a complex network of filaments released by the thecal pores (black arrowheads) and extracellular mucilage (white arrowheads). (E, F) Magnification on the apical dorsal part showing the apical pore plate Po; (E) intact Po (black arrowheads) and the plate 2'; (F) suture between the plate 2' and the Po which is missing (white arrowheads). Scale bars = 2 μm (A, B, C, D, and F); 5 μm (E).

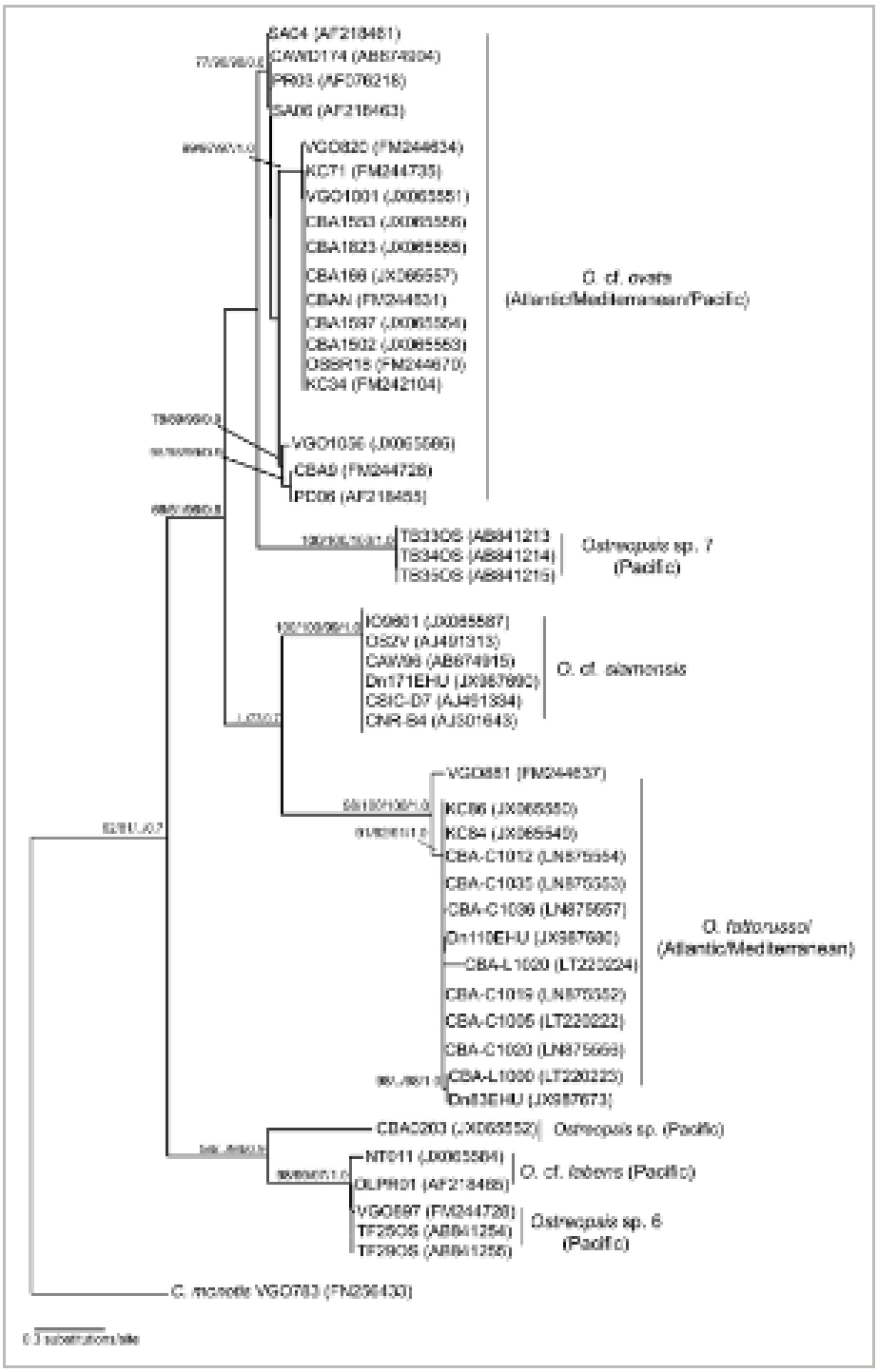

Figure 7

Open in figure viewer | PowerPoint

Maximum likelihood phylogenetic tree of the genus *Ostreopsis* inferred from ITS-5.8S ribosomal gene sequences. The tree is rooted with *Coolia monotis* VGO783 as outgroup. Numbers on the major nodes represent from left to right NJ (1,000 pseudo-replicates), MP (1,000 pseudo-replicates), ML (1,000 pseudo-replicates) bootstrap and Bayesian posterior probability values. Only bootstrap values >50% are shown. Geographical origins of *Ostreopsis* isolates are indicated.

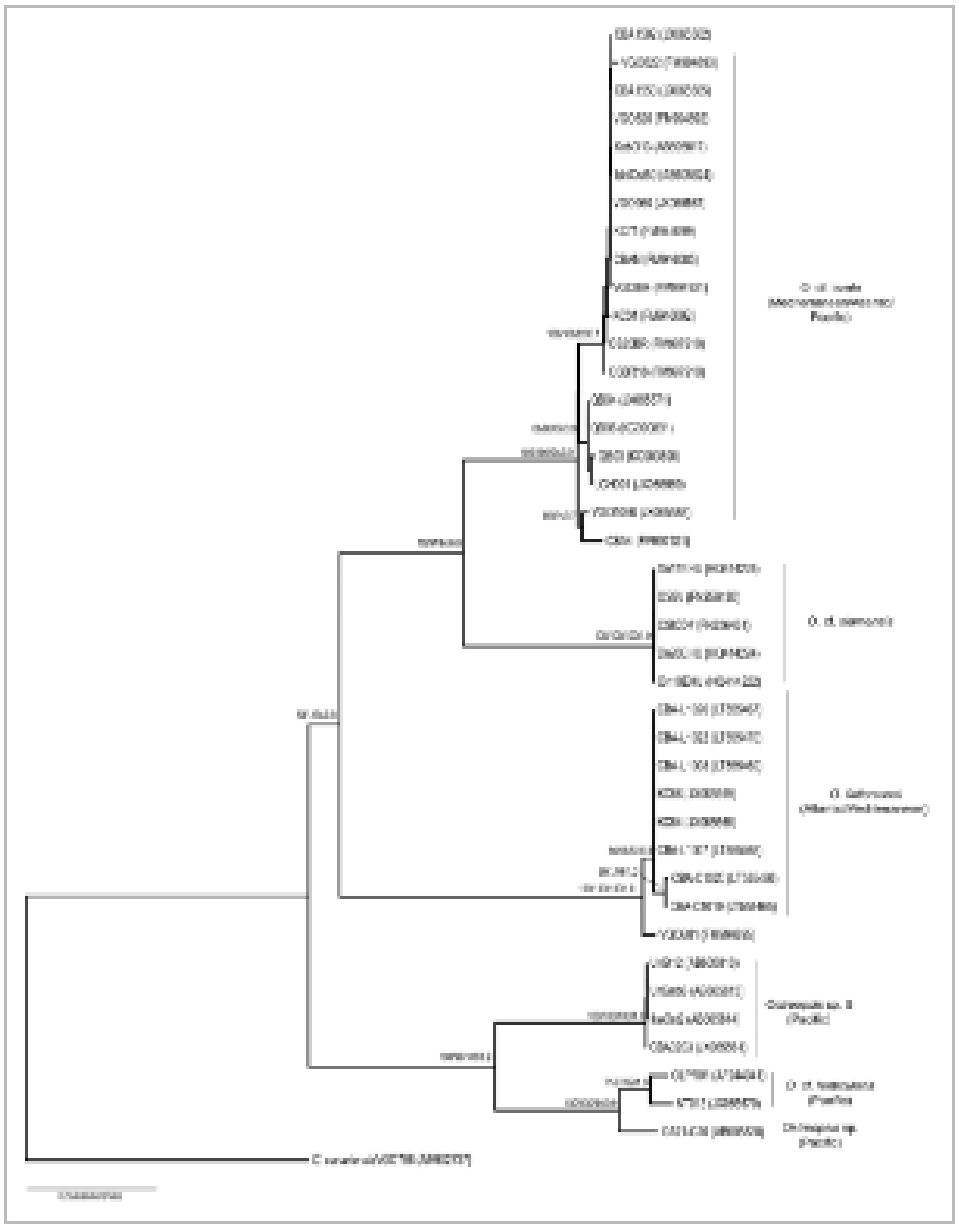

Figure 8 Open in figure viewer | PowerPoint

Maximum likelihood phylogenetic tree of the genus *Ostreopsis* inferred from LSU ribosomal gene sequences. The tree is rooted with *Coolia monotis* VGO786 as outgroup. Numbers on the major nodes represent from left to right NJ (1,000 pseudo-replicates), MP (1,000 pseudo-replicates), ML (1,000 pseudo-replicates) bootstrap and Bayesian posterior probability values. Only bootstrap values >50% are shown. Geographical origins of *Ostreopsis* isolates are indicated.

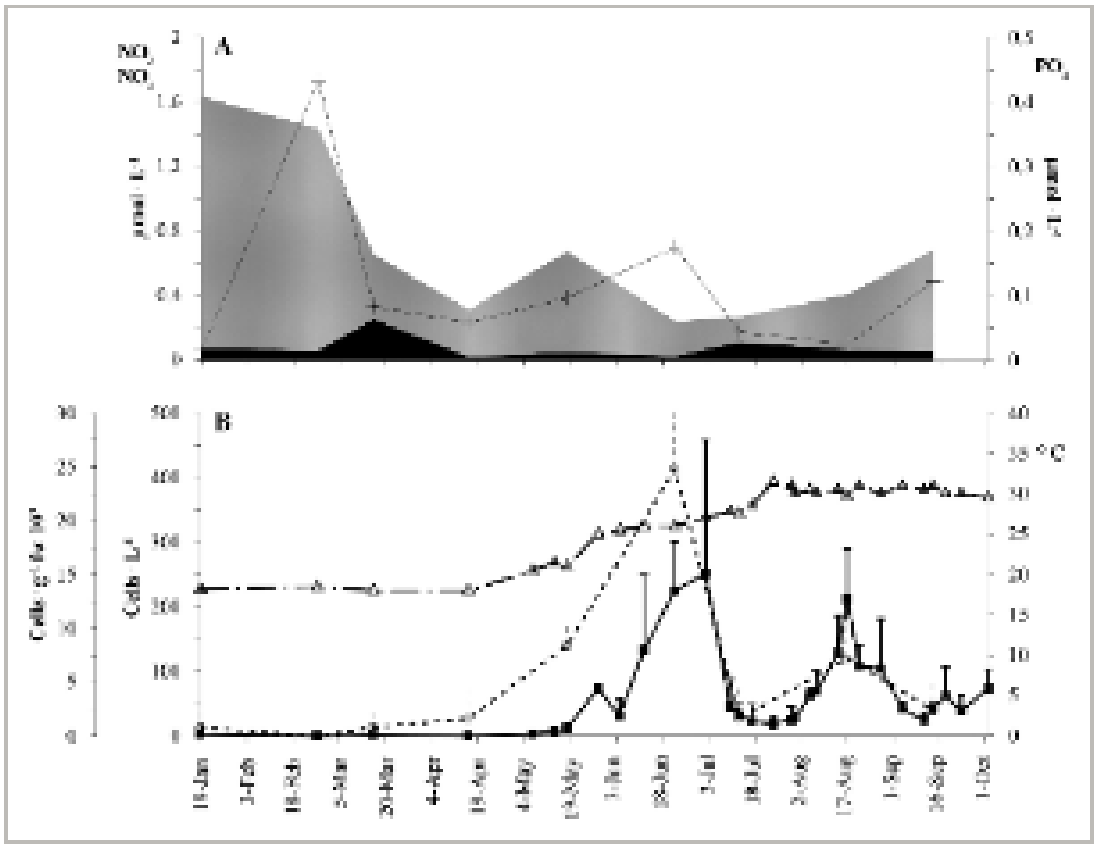

Figure 9

Trend in nutrient concentration, temperature and *Ostreopsis fattorussoi* abundances both on benthic macroalgae and in water column in Batroun (Lebanon) during 2015. (A) Nutrient concentration (µmol · L^{-1}): inorganic nitrogen with the detail of NO_3 and NO_2 (*gray* and black, respectively, left *y*-axis), and PO_4 (line, right *y*-axis). (B) *O. fattorussoi* abundances on seaweeds (▲, 1st left *y*-axis) and in the water column (○, 2nd left *y*-axis) expressed in cells · g^{-1} fw and cells · mL^{-1}, respectively. Temperature values expressed in °C (▲, right *y*-axis). Error bars indicate standard deviations.

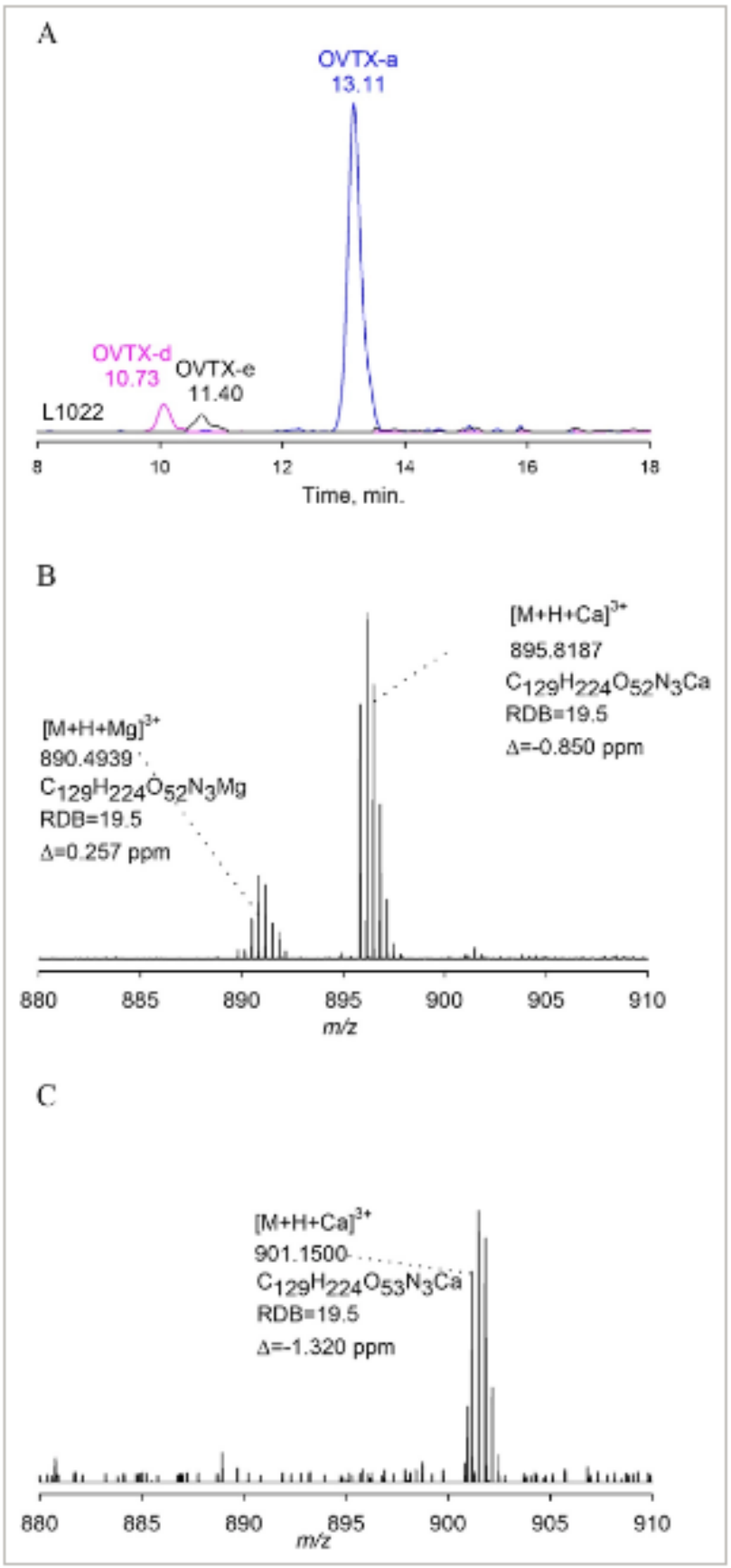

Figure 10

LC-HRMS analysis of *Ostreopsis fattorussoi* L1022 strain, including (A) extracted ion chromatogram (XIC) of $[M+H+Ca]^{3+}$ ions of ovatoxin-a (OVTX-a) and of the structural isomers ovatoxin-d and -e (OVTX-d, -e). Enlargements of the full HRMS spectra of (B) OVTX-a and (C) OVTX-d/-e.

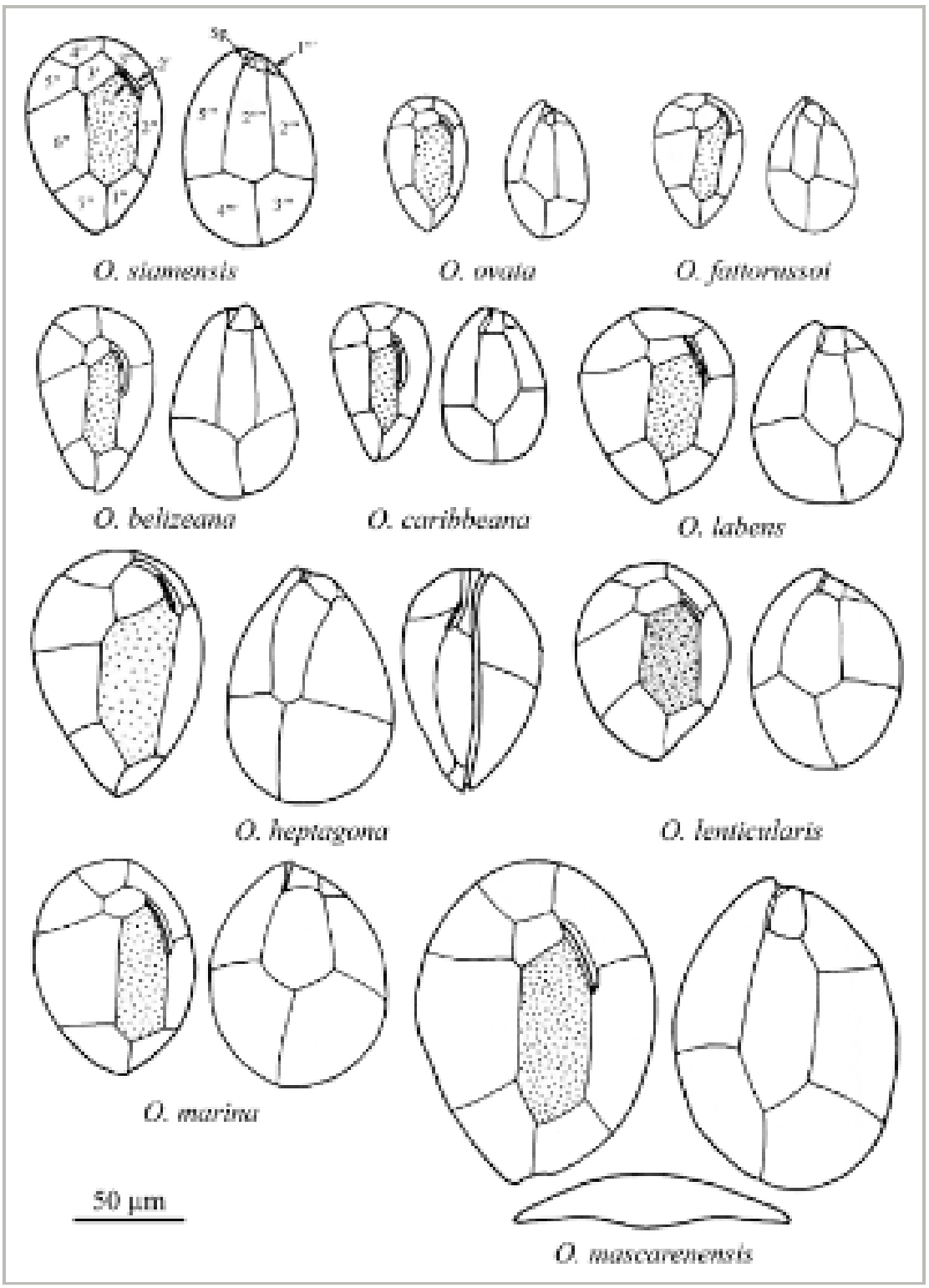

Figure 11

Drawings of the plate patterns of the ten described Ostreopsis spp. modified from Hoppenrath et al. (2014). All species to scale.

TABLE 1. List of *Ostreopsis* spp. isolates, sampling locations, isolator, ITS – 5.8S, and LSU gene sequence accession numbers from GenBank and EMBL.

Species	Strain ID	Geographical origin and collecting period	Isolator	Accession no. ITS-5.8S	Accession no. LSU
O. cf. ovata	CBA166	Trieste, Italy, Adriatic Sea, Mediterranean, 2009	Penna A.	JX065557	
O. cf. ovata	CBA1823	Taormina, Italy, Ionian Sea, Mediterranean, 2010	Battocchi C.	JX065555	
O. cf. ovata	CBA1597	Marina di Pisa, Italy, Tyrrhenian Sea, Mediterranean, 2010	Casabianca S.	JX065554	
O. cf. ovata	CBA1502	Alghero, Italy, Tyrrhenian Sea, Mediterranean, 2010	Capellacci S.	JX065553	JX065562
O. cf. ovata	CBA1553	Villefranche, Ligurian Sea, Mediterranean, France, 2010	Battocchi C.	JX065556	JX065565
O. cf. ovata	CBA N	Tyrrhenian, Mediterranean, Italy, 2007	Capellacci S.	FM244631	FM946085
O. cf. ovata	VGO 820	Catalan, Mediterranean, 2005	Fraga S.	FM244634	FM994892
O. cf. ovata	VGO 822	Catalan, Mediterranean, 2005	Fraga S.		FM994893
O. cf. ovata	VGO 884	Catalan, Mediterranean, 2005	Fraga S.		FM994931
O. cf. ovata	VGO960	Llavaneres, Spain, Catalan Sea, Mediterranean, 2008	Fraga S.		JX065567
O. cf. ovata	VGOOS20BR	Rio de Janeiro, Brazil, W Atlantic Ocean, 2000	Fraga S.		FM997919
O. cf. ovata	VGO1001	Famara, Canary Island, Spain, E Atlantic Ocean, 2008	Rodriguez F.	JX065551	
O. cf. ovata	VGO1056	Belize, Caribbean Sea, N Atlantic Ocean, 2009	Holland C.	JX065586	JX065588
O. cf. ovata	KC34	Aegean, Mediterrean, 2004	Aligizaki K.	FM242104	FM946092
O. cf. ovata	KC71	Aegean, Mediterrean, 2004	Aligizaki K	FM244735	FM946099
O. cf. ovata	OS18BR	West Atlantic, Brazil, 2000	Fraga S	FM244670	FM997918
O. cf. ovata	CBA4	East Pacific, Indonesia, 2007	Penna A.		FM997921
O. cf. ovata	CBA9	East Pacific, Indonesia, 2007	Penna A.	FM244726	
O. cf. ovata	OvPD06	Indian, Malaysia, 1997	Pin L.C.	AF218455	
O. cf. ovata	OvSA04	Indian, Malaysia, 1997	Pin L.C.	AF218461	
O. cf. ovata	PR-03	Indian, Malaysia, 1997	Pin L.C.	AF076218	
O. cf. ovata	OvSA06	Indian, Malaysia, 1997	Pin L.C.	AF218463	
O. cf. ovata	CAWD174	Rarotonga, Cook Island, 2009	Strickland R. Sellwood A.	AB674904	
O. cf. ovata	KabO13	Okinawa,Ishigaki, Kabira, Japan 2010	Suda S.		AB605817
O. cf. ovata	IshiOst50	Okinawa,Ishigaki, Shiraho,Japan, 2009	Shah M.R.		AB605824
O. cf. ovata	QB04	Quang Binh, Vietnam, South China Sea, Pacific, 2009	Nguyen N.L.		JX065571
O. cf. ovata	QB06	Quang Binh, Vietnam, South China Sea, Pacific, 2009	Nguyen N.L.		KC900891
O. cf. ovata	QB03	Quang Binh, Vietnam, South China Sea, Pacific, 2009	Nguyen N.L.		KC900890
O. cf. ovata	LCH001	Thua Thien-Hue, Vietnam South China Sea, Pacific, 2009	Nguyen N.L.		JX065569
O. cf. siamensis	IO-9601	Sines, Portugal, E Atlantic, 2008	Veloso V.	JX065587	
O. cf. siamensis	OS-2V	Alboran, Mediterranean, 1999	Fraga S	AJ491313	
O. cf. siamensis	OS-5V	Alboran, Mediterranean, 1999	Fraga S		FN256430
O. cf. siamensis	CSIC-D7	Catalan, Mediterranean, 2000	Garcés E.	AJ491334	FN256431
O. cf. siamensis	CNR-B4	Tyrrhenian Sea, Mediterranean, 2000	Giacobbe M.G.	AJ301643	
O. cf. siamensis	CAWD96	Kerikeri, New Zealand, 1999	North Health Services	AB674915	
O. cf. siamensis	Dn17EHU	Biscay, Spain, 2007–2009	Laza A.		HQ414225
O. cf. siamensis	Dn 20EHU	Biscay, Spain, 2007–2009	Laza A.		HQ414224
O. cf. siamensis	Dn18EHU	Biscay, Spain, 2007–2009	Laza A.		HQ414222
O. cf. siamensis	Dn171EHU	Saint Jean de Luz, France, 2010	David H.	JX987690	
O. cf. labens	VGO897	Indian, Malaysia, 1997	Mohammad N.	FM244728	
O. cf. lenticularis	NT011	Ninh Thuan, Vietnam, South China Sea, 2009	Nguyen N.L.	JX065584	
O. cf. lenticularis	NT013	Ninh Thuan, Vietnam, South China Sea, 2009	Nguyen N.L.		JX065570
O. cf. lenticularis	OLPR01	Indian, Malaysia, 1997	Pin L.C.	AF218465	AF244941
Ostreopsis sp.	TB34OS	Khao Lak, Phang-Nga, Thailand, 2015	Tawong W.	AB841214	
Ostreopsis sp.	TB35OS	Khao Lak, Phang-Nga, Thailand, 2015	Tawong W.	AB841215	
Ostreopsis sp.	TB33OS	Khao Lak, Phang-Nga,Thailand, 2015	Tawong W.	AB841213	
Ostreopsis sp.	KC84	Cyprus, Aegean Sea, Mediterranean, 2008	Aligizaki K.	JX065549	JX065558
Ostreopsis sp.	KC86	Crete, Greece, Aegean Sea, Mediterranean, 2009	Aligizaki K.	JX065550	JX065559
Ostreopsis sp.	CBA0203	Honolulu, Hawaii, N Pacific Ocean, USA, 2010	Capellacci S.	JX065552	JX065561
Ostreopsis sp.	VGO881	Canary Island, East Atlantic, 2005	Fraga S.	FM244637	FM994895
Ostreopsis sp.	Dn83EHU	Crete, Greece, 2010	David H.	JX987673	
Ostreopsis sp.	Dn110EHU	Puerto Rico, North America 2011	David H.	JX987680	
Ostreopsis sp.	TF29OS	Koh Wai, Trat, Thailand, 2011	Tomohiro N.	AB841255	
Ostreopsis sp.	TF25OS	Koh Wai, Trat, Thailand, 2011	Tomohiro N.	AB841254	
O. fattorussoi	CBA C1005	Cyprus, Aegean Sea, Mediterranean, 2013	Capellacci S.	LT220222	
O. fattorussoi	CBA C1012	Cyprus, Aegean Sea, Mediterranean, 2013	Capellacci S.	LN875554	
O. fattorussoi	CBA C1019	Cyprus, Aegean Sea, Mediterranean, 2013	Capellacci S.	LN875552	LT555465
O. fattorussoi	CBA C1020	Cyprus, Aegean Sea, Mediterranean, 2013	Capellacci S.	LN875556	LT555466

Species	Strain ID	Geographical origin and collecting period	Isolator	Accession no. ITS-5.8S	Accession no. LSU
O. fattorussoi	CBA C1035	Cyprus, Aegean Sea, Mediterranean, 2013	Capellacci S.	LN875553	
O. fattorussoi	CBA C1036	Cyprus, Aegean Sea, Mediterranean, 2013	Capellacci S.	LN875557	
O. fattorussoi	CBA L1000	Batroun, Lebanon, Mediterranean, 2014	Capellacci S.	LT220223	
O. fattorussoi	CBA L1020	Batroun, Lebanon, Mediterranean, 2014	Capellacci S.	LT220224	LT555467
O. fattorussoi	CBA L1007	Batroun, Lebanon, Mediterranean, 2014	Capellacci S.		LT555468
O. fattorussoi	CBA L1008	Batroun, Lebanon, Mediterranean, 2014	Capellacci S.		LT555469
O. fattorussoi	CBA L1022	Batroun, Lebanon, Mediterranean, 2014	Capellacci S.		LT555470
Ostreopsis sp.	UrGt12	Okinawa, Urasoe, off camp Kinser, Japan, 2009	Suda S.		AB605813
Ostreopsis sp.	UrGm6	Okinawa, Urasoe, off camp Kinser, Japan, 2009	Suda S.		AB605815
Ostreopsis sp.	IkeOst2	Ikeijima, Uruma, Okinawa, Japan 2008	Suda S.		AB605814
Ostreopsis sp.	OA21-C10	Okinawajima Island, Japan	Nakashima A.		AB605828

TABLE 2. LC-HRMS analyses of *Ostreopsis fattorussoi* strains from Lebanon.

	Toxin content (pg · cell $^{-1}$)	Relative intensities		
		OVTX-a	OVTX-d	OVTX-e
L1002	nd	–	–	–
L1007	0.28	81.6%	11.7%	6.7%
L1008	nd	–	–	–
L1020	0.47	86.7%	8.8%	4.5%
L1022	0.94	87.8%	7.7%	4.5%

TABLE 3. Different interpretations of plate tabulation in *Ostreopsis* of different authors. n.r., not reported.

	Besada et al. (1982), Escalera et al. (2014)	Norris et al. (1985), Faust et al. (1996)	Hoppenrath et al. (2014)
Epitheca	Po (pp)	Po	Po
	4′	1′	1′
	2′	2′	2′
	3′	3′	3′
	1′	1″	1″
	1″	2″	2″
	2″	3″	3″
	3″	4″	4″
	4″	5″	5″
	5″	6″	6″
	6″	7″	7″
Hypotheca	1‴	1‴	1‴
	2‴	2‴	2‴
	3‴	3‴	3‴
	4‴	4‴	4‴
	5‴	5‴	5‴
	1⁗	1⁗	1⁗
	2⁗	1p	2⁗
Cingulum	n.r.	n.r.	1c
	n.r.	n.r.	2c
	n.r.	n.r.	3c
	n.r.	n.r.	4c
	n.r.	n.r.	5c
	n.r.	n.r.	6c
Sulcus	n.r.	n.r.	Sa
	n.r.	n.r.	Sda
	n.r.	n.r.	Ssa
	n.r.	n.r.	S.ac.a
	n.r.	n.r.	Sdp
	n.r.	n.r.	Ssp
	ps	n.r.	Sp

TABLE 4. Comparison of morphometric parameters of *Ostreopsis siamensis*, *O. ovata*, *O.* cf. *siamensis*, *O.* cf. *ovata*, and *O. fattorussoi* based on measurements of specimens from literature values and this study.

Species	Apical pore (μm)	Pore size in thecal plates (μm)	Reference
O. fattorussoi sp.nov.	10–12.5 (11.7 ± 1.4)	0.26–0.53 (0.38 ± 0.08)	This study
O. siamensis Schmidt	27	0.1–0.5	Faust et al. 1996,
		0.08–0.38	Chang et al. 2000,
O. cf. *siamensis*	7.4–9.7	0.11–0.56 (0.30 ± 0.07)	Penna et al. 2005,
	10.9 ± 1.24	0.23–0.29	Aligizaki and Nikolaidis 2006,
	11–13	0.14–0.32	Selina and Orlova 2010,
O. ovata Fukuyo	8	0.07	Faust et al. 1996,
	6.9–9.6	0.16–0.55 (0.34 ± 0.10)	Penna et al. 2005,
	10.9 ± 0.77	0.07–0.32	Aligizaki and Nikolaidis 2006,
O. cf. *ovata*	6.6–9.0	0.25	Monti et al. 2007,
	6.3–8.3	0.12–0.25	Selina and Orlova 2010,
	4.8–6.8	0.06–0.26	Kang et al. 2013

[Correction added on December 2, 2016, after first online publication: page 15, at the end of 3rd paragraph, pentagonal changed to heptagonal].